

Temporal change detection of mangrove species utilizing Sentinel-2 Satellite data for various study sites in India.

A Thesis

submitted to

Indian Institute of Science Education and Research Pune

in partial fulfilment of the requirements for the

BS-MS Dual Degree Programme

by

Aby K Mathai



Indian Institute of Science Education and Research Pune

Dr. Homi Bhabha Road, Pashan,

Pune 411008, INDIA.

December 2023

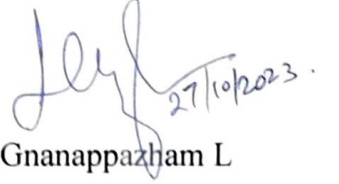
Supervisor: Dr. Gnanappazham L.

© Aby K Mathai 2023

All rights reserved

Certificate

This is to certify that this dissertation entitled **Temporal change detection in mangrove utilizing Sentinel-2 Satellite data for various study sites in India** towards the partial fulfilment of the BS-MS dual degree programme at the Indian Institute of Science Education and Research, Pune represents study/work carried out by Aby K Mathai at Indian Institute of Space Science and Technology, Trivandrum under the supervision of Gnanappazham L, Professor, Department of Earth and Space Science, during the academic year 2022-2023.



Dr. Gnanappazham L

Committee:

Dr. Gnanappazham L (Earth and Space Science, IIST Trivandrum)

Dr. Sudipta Sarkar (Earth & Climate Science, IISER Pune)

डॉ. एल ग्नापपझम / Dr. Gnanappazham
आचार्य Professor
पृथ्वी एवं अंतरिक्ष विज्ञान विभाग
Department of Earth and Space Sciences
भारतीय अंतरिक्ष विज्ञान एवं प्रौद्योगिकी संस्थान
Indian Institute of Space Science and Technology
अंतरिक्ष विभाग, भारत सरकार
Dept. of Space, Govt. of India
तिरुवनंतपुरम / Thiruvananthapuram - 695 547

Dedicated to my Appa, Amma, Mikku.

To Dear friend Reshmi.

Declaration

I hereby declare that the matter embodied in the report entitled **Temporal change detection in mangrove utilizing Sentinel-2 Satellite data for various study sites in India** are the results of the work carried out by me at the Department of Earth and Space Science, Indian Institute of Space Science and Technology, Trivandrum, under the supervision of Dr. Gnanappazham L and the same has not been submitted elsewhere for any other degree.



Aby K Mathai

Date: 31/10/2023

Table of Contents

Declaration.....	4
Abstract.....	11
Acknowledgments.....	12
Chapter 1 Introduction.....	13
1.1 Remote sensing.....	13
1.2 Mangroves.....	13
1.3 Sentinel-2.....	15
1.4 Reflectance spectra of leaf.....	16
1.5 Study sites.....	18
1.6 Materials.....	19
1.6.1 Computational requirements.....	20
1.6.2 Spectral data collection requirements.....	20
Chapter 2 Methodology.....	21
2.1 Preprocessing of images.....	21
2.2 Preliminary analysis.....	22
2.3 JM distance.....	22
2.4 Supervised Classification.....	23
2.5 Change analysis.....	23
2.6 Spectral data collection.....	24
2.6.1 Field data collection.....	24
2.6.2 Laboratory data collection.....	25
2.7 Spectral data Post-processing.....	25
2.7.1 Drift correction or splice correction.....	25
2.7.2 Removal of water absorption bands and unilluminated bands.....	26
2.7.3 Smoothing of reflectance spectra.....	27
2.7.4 Resampling hyperspectral data to Sentinel 2 spectral resolution.....	27
2.8 Ground Truths (GTs) data collection.....	28
Chapter 3 Results and Discussion.....	29
3.1 Reflectance spectra collected by onsite field visits.....	29
3.2 Thane.....	34
3.3 Sadamirya.....	39
3.4 Bhitarkanika.....	44
3.5 Lothian Island.....	52
3.6 Pichavaram.....	58
3.7 Malad.....	63
Chapter 4 Conclusion.....	69

List of Tables

Table number	Caption	Page number
1.1	Sentinel - 2 bands with spatial resolution.	16
3.1	Species identified in different study sites and the source of data.	33
3.2.1	Land cover of different mangrove species: Thane region	36
3.2.2	Accuracy assessment for Thane region.	36
3.2.3	JM distance matrix for Thane.	36
3.3.1	Accuracy assessment: Sadamirya region	42
3.3.2	JM distance matrix for Sadamirya.	42
3.3.3	Land cover of different mangrove species: Sadamirya region.	42
3.4.1	Accuracy assessment: Bhitarkanika	47
3.4.2	JM distance matrix for Bhitarkanika.	47
3.4.3	Land cover of different mangrove species: Bhitarkanika region	48
3.5.1	Accuracy assessment: Lothian Island	54
3.5.2	JM distance matrix for Lothian Island.	54
3.5.3	Land cover of different mangrove species: Lothian Island.	55
3.6.1	Accuracy assessment: Pichavaram	61
3.6.2	JM distance matrix for Pichavaram.	61
3.6.3	Land cover of different mangrove species: Pichavaram.	61

3.7.1	Accuracy assessment: Malad.	66
3.7.2	JM distance matrix for Malad.	66
3.7.3	Land cover of different mangrove species: Malad region.	66

List of Figures

Figure number	Caption	Page number
1.1	Mangrove forest in Gorai region, Mumbai, India. Image captured during low tide. In the image, pneumatophores, and different species of mangroves such as <i>Avicennia marina</i> in the form of big trees and an associated mangrove <i>Acanthus ilicifolius</i> seen growing under the canopy can be seen.	15
1.2	Spectral reflectance curve for few earth surface materials (John, 1993).	17
1.3	Study sites shown in standard FCC with respect to given scale (R: NIR, G: Red, B: Green).	18
2.1	Flowchart of methodology adopted.	21
2.2	Laboratory ASD data collection setup.	25
2.3	Enhanced view of reflectance data at 1001 nm to demonstrate the change in reflectance spectra before and after splice correction.	26
2.4	Typical field setting ASD spectral data demonstrating atmospheric window region and the absorption band region of electromagnetic spectrum.	27
2.5	GT points and transect survey done for Thane region. (Survey transect is shown in red line).	28
3.1.1	Reflectance spectra collected from field surveys. Post processed hyperspectral data is shown in the figure.	30
3.1.2	West coast ASD reflectance data resampled to Sentinel 2 resolution and compared to study sites along west coast. (For thane region the legends are different than other images.)	31
3.1.3	East coast ASD reflectance data resampled to Sentinel 2 resolution and compared to study sites along east coast.	32
3.2.1	Color composites of Thane study.	35

3.2.2	Classification outputs for Thane site.	35
3.2.3	Yearly data for November 2015 - 2022 for Band 6, Band 7, Band 8, Band 8A (RE4) and Band 11 for Thane.	37
3.2.4	NDVI changes through study years for Thane site.	38
3.2.5	NDVI seasonal trend from 2016 – 2023 for the two mangrove classes in Thane region.	39
3.3.1	Different band combinations for Sadamirya study site.	40
3.3.2	Classification output for Sadamirya site.	41
3.3.3	NDVI Changes through years for Sadamirya site.	41
3.3.4	Yearly data for November 2016 - 2022 for Band 6, Band 7, Band 8, Band 8A, Band 11 for Sadamirya.	43
3.3.5	NDVI seasonal trend from 2016 – 2022 for each species of Sadamirya.	44
3.4.1	Color composites of Bhitarkanika study site.	46
3.4.2	Classification output using Sentinel-2 L1C product. 2016 December image and 2022 November image considered for classification of the respective years.	46
3.4.3	Yearly December data for Band 6, Band 7, Band 8, Band 8A, Band 11 from 2016 – 2022 for Bhitarkanika.	49
3.4.4	NDVI image of December 2016 – 2022 with range.	50
3.4.5	NDVI seasonal trend from 2016 – 2023 for each species of Bhitarkanika.	51
3.5.1	Color composites of Lothian Island study site.	53
3.5.2	Classification outputs using RF for February 2019 and February 2023 for Lothian Island site.	53
3.5.3	Yearly data of February 2019 - 2023 for Band 6, Band 7, Band 8, Band 8A, Band 11 for Lothian Island.	56
3.5.4	NDVI yearly trend for February from 2019-2023 for Lothian Island.	57
3.5.5	NDVI image of February 2019 – 2023 with range for Lothian Island.	57
3.5.6	NDVI seasonal trend from 2019 – 2023 for each species of Lothian Island.	58
3.6.1	Different band combinations for Pichavaram study site. Image with scale and North arrow is standard FCC.	60
3.6.2	Classification output for Pichavaram site.	60
3.6.3	Figure 3.6.3. Yearly data of March 2019 - 2023 for Band 6, Band 7, Band 8, Band 8A, Band 11 for Pichavaram.	62

3.6.4	NDVI seasonal trend from 2019 – 2023 for each species of Pichavaram.	63
3.6.5	NDVI image of March 2016 – 2022 with range for Pichavaram.	63
3.7.1	Different band combinations for Malad study site.	65
3.7.2	Classification outputs for Malad site.	65
3.7.3	Yearly data of November 2019 - 2023 for Band 6, Band 7, Band 8, Band 8A, Band 11 for Malad site.	67
3.7.4	NDVI seasonal trend from 2019 – 2023 for each species of Malad.	68
3.7.5	NDVI image of November 2019 – 2022 with range for Malad.	68

List of Abbreviations:

ROI	Region of Interest
JM	Jeffries - Matusitta
ASD	Analytical Spectral Devices
GEE	Google Earth Engine
ENVI	ENvironment for Visualizing Images
RE	Red Edge
NIR	Near Infrared
SWIR	Short wave Infrared
GT	Ground Truth
FCC	False color composite
ML	Machine Learning
RF	Random Forest
NDVI	Normalized Difference Vegetation Index
EMR	Electromagnetic Radiation
PC	Personal Computer
AM	<i>Avicennia marina</i>
AA	<i>Avicennia alba</i>
AO	<i>Avicennia officinalis</i>

AR	<i>Aegialitis rotundifolia</i>
HF	<i>Heritiera fomes</i>
EA	<i>Excoecaria agallocha</i>
RH	<i>Rhizophora</i> sp.
RM	<i>Rhizophora mucronata</i>
SA	<i>Sonneratia alba</i>
CT	<i>Ceriops tagal</i>
CD	<i>Ceriops decandra</i>
PP	<i>Phoenix paludosa</i>
MX	Mixed species
TV	Terrestrial vegetation

Abstract

The mangrove ecosystem, considered fragile, requires regular monitoring due to its crucial role in coastal ecosystems. This study focuses on conducting a detailed, species-level analysis of mangrove vegetation over time, utilizing moderately high-resolution Sentinel-2 satellite data. Supervised classification utilizing Random Forest (RF) algorithm was used to discriminate mangrove vegetation on a species level. Upon investigation we could find the east coast mangroves have a higher species diversity compared to west coast. Only two true mangrove species such as *Avicennia marina* and *Rhizophora mucronate* were common mangrove species for each coast. The exceptional spatial and temporal resolution of Sentinel 2 has proven crucial in detecting nuanced alterations in land cover that would have otherwise been challenging to identify using conventional approaches. The field hyperspectral data collected used as the reference spectra gives insights to the reflectance spectra of these mangrove vegetation. Although most of the sites studied shows a conservation in mangrove vegetation, it is observed that few stands of mangroves are converted to other mixed mangrove patches within the study time. In study sites such as Thane and Pichavaram, a decrease in the mangrove vegetation cover accompanied by mud deposition was observed. In the Indian Sundarban site Lothian Island, the occurrence of new stands of vegetation was observed. Validation of the study is conducted by field surveys and visualization using google earth pro. Species mapping is done by Ground Truths (GTs) reported by onsite visits and studying the existing literature. Normalised Difference Vegetation Index (NDVI), changes are monitored for the study years, both seasonally and yearly to conclude on the health of vegetation and to correlate with the changes.

Acknowledgments

I would like to extend my sincere gratitude to Dr. Gnanappazham Lakshmanan who has given me this opportunity to work in the Remote Sensing lab, Earth and Space Science department, Indian Institute of Space Science and Technology, Trivandrum.

Throughout my time in this institute, I was able to attend workshops, classes and conferences on the subject. I am grateful in having the chance to meet many people during this period in and out of campus.

I am thankful to Dr. Sudipta Sarkar, Earth and Climate Science Department, IISER Pune who have been an inspiration and encouraged me to take up this project.

Finally, I would like to extend my thanks to my parents who have been there supporting me on this endeavour.

Chapter 1 Introduction

1.1 Remote sensing

Remote sensing (RS), as the term suggests, is acquiring information of a feature without being in physical contact with it. Recent studies have utilized images captured through smartphones, as well as LiDAR sensors in iPhones for inaccessible areas (Luetzenburg et al., 2021) emphasizing the potential of RS. Cameras mounted on satellites to sonar systems on ships are examples of remote sensing. Satellites have advanced cameras that can detect reflected or emitted electromagnetic radiation (EMR) within and beyond the visible region of the electromagnetic spectrum, typically in the Optical range (300-3000 nm). Every body whose temperature lies above zero kelvin radiates energy in the form of electromagnetic radiation (Stephan Boltzman law). Within the last five decades, there has been a boom in satellite technology with the evolution of high performance computing. From the initial days of capturing 60 m resolution images using Landsat satellites, the technology has advanced much to have spatial resolution below 1m, making monitoring of conservation sites easier.

1.2 Mangroves

Mangrove ecosystems, referred to as 'tidal forests', lie in the intertidal zones of coastlines. These woody halophytes comprise taxonomically diverse shrubs and trees distributed along tropical and subtropical environments. They are among one of the most productive ecosystems in the world as they provide essential ecosystem supplies and services to human society as well as coastal and marine systems. These forests act as buffers between land and ocean, absorbing wave action and preventing erosion (Saintilan et al., 2023). They play a major role in stabilizing the shoreline and protecting the coastal community from the coastal hazards like cyclone and tsunami (Gnanappazham & Selvam, 2014).

Economically these forests are a tourist attraction due to its species diversity and serenity. Mangrove tourism has provided the local community a means of livelihood. They live in close association with mangroves and are familiar with scientific names of each species of mangroves with their leaf size, shape, zonation and overall tree

height. There were newspaper articles on how women in Maharashtra play a good role in helping save these ecosystems, while they find a means of livelihood through mangrove tourism (Times of India, July 2, 2023). These forests provide timber, honey and are a platform for shrimp farming, and crabs found in the hummocks and hollows are a source of livelihood. It has been reported that farmers do shrimp farming with leaf litter of mangroves in West Bengal India (The Hindu, July 30, 2023), and studies are done to optimize these farming techniques as done in Nam Dinh Province, red river delta, Vietnam (Mai et al., 2023). These forests are potential breeding places for fishes, home for crabs to tigers, and a variety of birds.

Ecologically mangroves are important for enhancing the fishery production of the wetland system and also enriching the nearby coastal water by exporting the detritus from the forest through tidal action. Mangrove forests compared to any other forests outperform when it comes to sequestering atmospheric CO₂ (Yancho et al., 2020, Gnanappazham & Selvam, 2014, Nagarajan et al., 2022). They are 4-5 times more efficient than a tropical forest in the rate of carbon sequestration. Mangrove extent are an indicator of sea level rise, with relative sea level rise these ecosystems retreat the buffered area and vice versa. Recent study on Nature (Saintilan et al., 2023) says that with the current rate of sea level rise there is a potential risk of shrinking of these coastal habitats.

Mangroves are present along the Indian coastline. These forests occur mainly in the Indian states of Gujarat, Maharashtra, Goa, Karnataka, Kerala, Tamil Nadu, Andhra Pradesh, Odisha, and West Bengal. Species diversity of mangroves is higher in the East coast, called Deltaic mangroves in comparison to the West coast called Estuarine and Backwater mangroves (Pandisamy et al., 2016). India has been reported for holding the fourth largest mangrove cover in the world. 60 species of mangroves belonging to 41 genera and 29 families have been reported (Neethu and Harilal, 2018). While the importance of monitoring mangroves are apparent, there have been fewer studies on temporal changes on Indian mangroves. Most of the studies that have been conducted utilizes Landsat imagery for time series study as it has multidecadal data. When it comes to species level mangrove mapping, while we compromise on spectral resolution, the spatial resolution must be sufficient to distinguish between different mangroves. Biodiversity hotspots such as mangrove ecosystems are prone to human encroachment and to natural stresses. These can

affect the total population of mangroves and these need to be addressed. RS provide a solution to the expensive and time consuming field surveys as they provide a way to monitor forests on a larger spatial scale (Nagarajan et al., 2022).



Figure 1.1. Mangrove forest in Gorai region, Mumbai, India. Image captured during low tide. In the image, pneumatophores, and different species of mangroves such as *Avicennia marina* in the form of big trees and an associated mangrove *Acanthus ilicifolius* seen growing under the canopy can be seen.

1.3 Sentinel-2

An initiative of Europe's Copernicus program, Sentinel-2 satellites since its launch in 2015 provide a global coverage of land use, land cover monitoring with a moderately high resolution of 10 m pixel size. Sentinel-2 is a multispectral sun-synchronous satellite with 13 bands as given below. As these images are open source and have a revisit time (temporal resolution) of 5-6 days, these provide a cheap way to monitor land resources.

Table 1.1 Sentinel - 2 bands with spatial resolution.

Band	Description	Central wavelength (nm)	Bandwidth (nm)	Spatial resolution (m)
B1	Aerosols	443	20	60
B2	Blue	497	65	10
B3	Green	560	35	10
B4	Red	665	30	10
B5	Red Edge 1	704	14	20
B6	Red Edge 2	740	14	20
B7	Red Edge 3	783	19	20
B8	NIR	835	105	10
B8A	Red Edge 4	865	21	20
B9	Water vapor	945	20	60
B10	Cirrus	1375	30	60
B11	SWIR 1	1614	90	20
B12	SWIR 2	2202	174	20

1.4 Reflectance spectra of leaf

Plant reflectance curve shows low values in the blue region, followed by a peak in the visible green region, then there is a fall in the red region due to absorption by leaf chlorophyll. From the Red part of the spectrum, there is an abrupt increase in reflectance to the Infrared region, referred to as the Red Edge (RE). This is typical of healthy leaf spectra. The RE is used to distinguish different species of plants, hence it is of most importance in the whole of leaf spectra. The higher reflectance in the Near Infrared (NIR) region in the leaf is due to the cell walls and the structure.

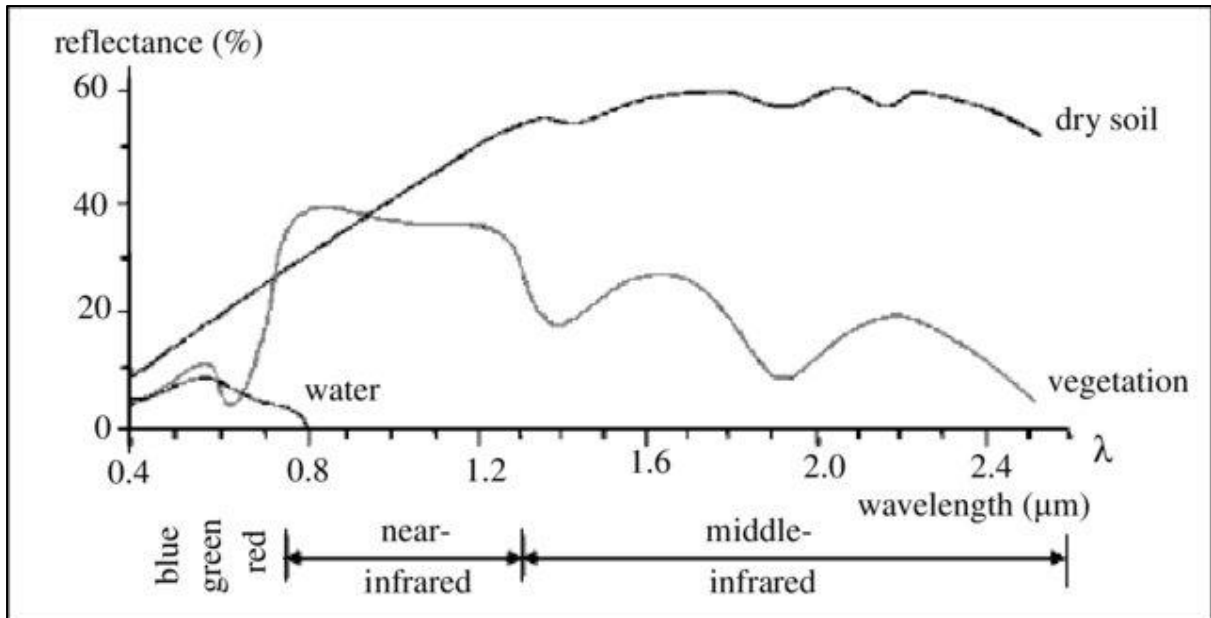


Figure 1.2. Spectral reflectance curve for few earth surface materials (John, 1993).

It can be seen that water plays an important role in absorption at the short wave Infrared (SWIR) portion of the spectrum. So, in burnt plants or dry plants this water absorption would not be present which makes the spectra look more like a soil spectrum. The nature of how the earth materials transmit, absorb or reflect the solar EMR is called spectral signature of an object. The fact that the spectral signature of any material is unique can be effectively utilized to distinguish and identify objects.

1.5 Study sites

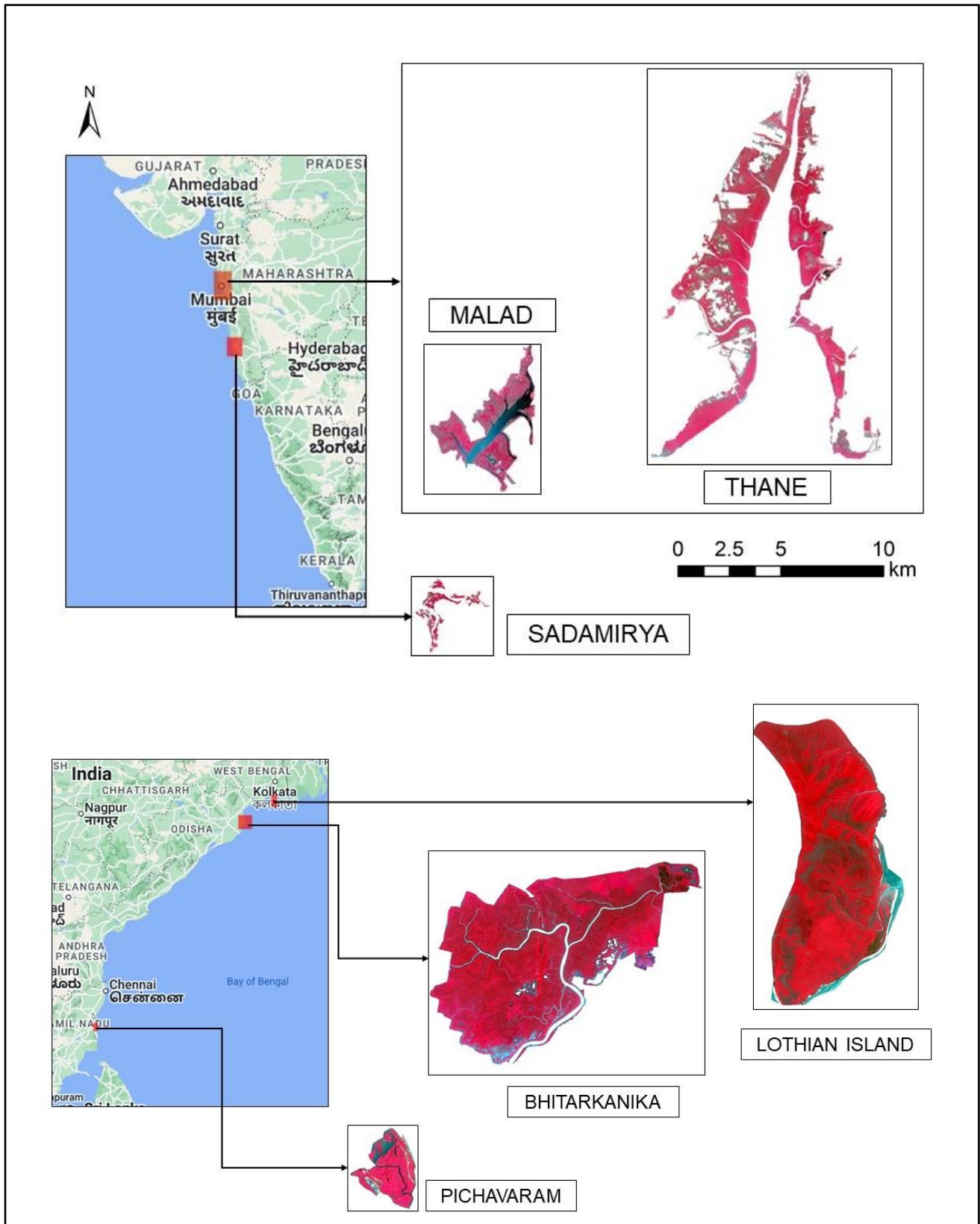


Figure 1.3 Study sites shown in standard FCC with respect to given scale (R: NIR, G: Red, B: Green).

Thane (Maharashtra): The region is situated between latitudes 18° 48' to 19° 12' N and longitudes 72° 48' to 73° 00' E. This area exhibits the presence of mangrove species such as *Avicennia marina*, *Bruguiera cylindrica*, *Sonneratia apetala*, where *Avicennia marina* is the dominant species in the region.

Sadamirya (Maharashtra): This region is situated between the latitudes 16° 59' to 17° 3' N and longitudes 73° 16' to 73° 19' E.

Bhitarkanika (Odisha): It is in Kendrapada district, Odisha. The study area extends from latitudes of 20.51°–20.85°N and longitudes of 86.75°–87.2°E. The major mangrove species in this region includes *Heritiera fomes*, *Excoecaria agallocha*, and *Avicennia officinalis*.

Lothian Island (West Bengal): Wildlife Sanctuary of Sundarbans Biosphere, West Bengal, located between latitudes of 21°49' to 21°32' N and longitudes 88°10' to 88°21' E.

Pichavaram (Tamil Nadu): The region extends from 11°20' N to 11°30' N latitude and 79°45' E to 79°50' E longitude. The dominant mangrove species found in this region include *Rhizophora sp.* (RH) and *Avicennia marina* (AM), where AM can be found in dense and moderately dense patches.

Malad (Maharashtra): The study area is located between the Latitudes 19°7'48", 19°11'55" N and Longitudes 72°47'13", 72°50'2"E . The most abundant mangrove species found in Malad creek is *Avicennia marina*, commonly called as grey mangrove. Other species found include *Sonneratia apetala* and *Rhizophora mucronate* but in few stands.

1.6 Materials

For this study, most of the work was done using a Personal Computer (PC) with an internet connection. In addition to the computational work, the spectral data for mangrove species present in west coast of India was collected using ASD FieldSpec® 3 spectroradiometer. For study purpose, spectral library of mangrove species along the East coast of India was provided from IIST.

1.6.1 Computational requirements

Since Google Earth Engine (GEE), an open source cloud-based platform was used for satellite image processing and analysis, a stable internet connection and enough space in Google Drive were required. For data visualization and plotting, python programming language was used. Other geospatial analysis software such as ArcMap and ENVI (ENvironment for Visualizing Images) which are not open-sourced were also put into use.

GEE has been used extensively for remote sensing studies as it is open source platform to anyone with a google account for scientific studies, its availability to be used in a personal computer with good internet connection as well as its radiometrically and geometrically corrected Landsat archive which could be used for multi decade time series studies (Yancho et al, 2020). This platform works in JavaScript API, while one can work on server, it provides users the functionality to download multispectral satellite images of Sentinel, Landsat, hyperspectral images of Hyperion as well as digital elevation data acquired using SRTM satellites for offline analysis.

1.6.2 Spectral data collection requirements

Spectral data collection was done using ASD FieldSpec® 3 spectroradiometer which has a spectral range of 350-2500 nm and sampling interval of 1.4 nm at 350-1050 nm and 2 nm at 1000-2500 nm (ASD 2010). RS³ software for ASD installed in a laptop was used for fieldwork. Additionally for Laboratory data collection, Tripods, halogen lamp and black cloth were required.

Chapter 2 Methodology

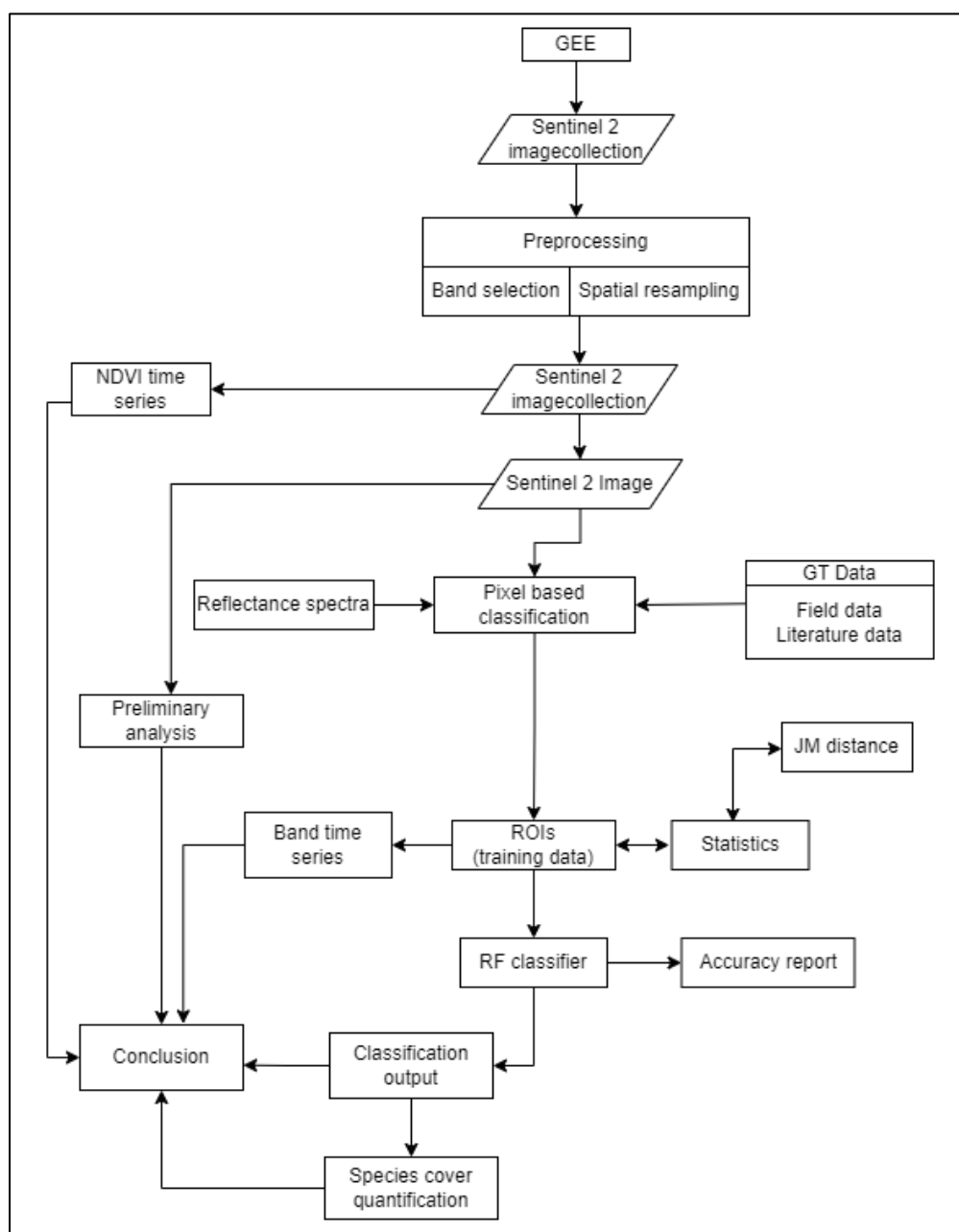


Figure 2.1. Flowchart of methodology adopted.

2.1 Preprocessing of images

Among the 13 bands in Sentinel 2 image, only 10 bands are used for study. These bands belong to visible, Red Edge, NIR and SWIR regions. Since these bands are of different spatial resolution, spatial resampling to 10 m resolution is carried out. Images are clipped to the study area. Only cloud free images are selected for study purposes, and although algorithms exist to create a mean cloud free image of our

region of interest, the approach taken here is manually verifying each image to be cloud free. There are 2 levels of satellite images taken for the study. These are raw images which are not atmospherically corrected called Top of atmosphere reflectance image (Level 1C) and the other set of images include atmospherically corrected Bottom of atmosphere reflectance images, level 2A image sets. Level 1C images have reflectance values affected by the atmosphere scattering and hence there would be likely attenuation of reflectance data received in the satellite sensors. Level 2A products are made from these 1C products by processing them using Sen2cor algorithm.

2.2 Preliminary analysis

The Sentinel 2 Multispectral data of the selected study areas were visually analyzed to understand the vegetation types and its distribution using various band combination. The band combinations given below are some of the standard composites used in different field (Source: GIS Geography). These composites are made on spatial resampled images.

1. Standard FCC uses NIR, Red and Green bands respectively for RGB channels. This composite is made in order to highlight the vegetation of an area.
2. Geology uses SWIR2, SWIR1, and blue bands respectively for the Red, Green, Blue channels. Primarily this combination is used by geologists for applications in finding faults and features.
3. SWIR combination uses SWIR2, Red Edge 4, and Red respectively for RGB channels. This combination primarily distinguishes denser vegetation as dark green from sparse vegetation. Mud and water appear as brown and blue respectively in this band combination.
4. Agriculture combination uses SWIR1, NIR and Red respectively for RGB channels, and this combination works similar to SWIR band combination.

2.3 JM distance

This is a statistical parameter commonly used in satellite data analysis to measure the spectral separability between two classes. The range of this parameter is from zero to two, two indicating the ROIs have excellent separability. A JM distance value

below one indicates the need to consider the ROIs as a single class (Richards 1999, Jeffreys, 1944). The threshold to separate ROIs is subjective and lies between one and two. Most studies consider ROIs with JM distance value below 1.8 to be merged to a single class.

2.4 Supervised Classification

The Mangrove patches of different species can be visualized with the help of crown size, their zonation, these serve as the initial GT. Training data for supervised classification is done by selecting homogenous patches of mangrove vegetation by visually interpreting the image in standard False Color Composite, and by inspecting the reflectance spectra of selected regions. Terrestrial vegetation and mangrove vegetation are detected and separated using the SWIR region of reflectance spectra, while the mangrove classes are separated on their difference mainly in the Red Edge and NIR band region. Multiple classes are made by collecting the endmember spectra based on the reflectance values in the mangrove distinguishing bands, and the initial label is chosen based on a statistical parameter JM distance (Dabboor, et al., 2014, Campos-Taberner et al., 2019) used for evaluating spectral separability. If two classes are having a JM distance below 1, it is merged into a single class. With the GT data and the field reflectance spectra, the classes (training data) are identified as different mangrove species. Pixel based supervised classification approach is performed using a robust ML algorithm Random Forest. For moderate resolution satellite images such as that of Sentinel-2, Pixel based supervised classification approaches have proven to provide accurate results as studies done by H. Sanam (Sanam et al., 2023).

2.5 Change analysis

The time series study approach is done by making use of the selected Region of Interest (ROI) statistics over time. Interpreting the trends in those bands which help in distinguishing between species is analyzed. The health of each species is analyzed using NDVI during the same month of each year. The higher the NDVI value, the healthier the vegetation and vice versa. The seasonal changes in vegetation across the study years is also studied. The initial image and final image are classified using the same ROI from the respective images and the differences

are analyzed and interpreted. The areal extent of species class from each classification image is calculated and is used to correlate with the observations. This quantification helps in the extent to which the changes might have happened.

Mangrove species discrimination is possible with Green and NIR wavelength regions (Viennois et al., 2016). A forest ecosystem can be quite heterogeneous and difficult to read from a satellite image. Since mangroves are the transition zones from land to ocean ecosystems, terrestrial vegetation could be seen in patches within the mangrove forests. For the purpose of mapping mangroves from the rest of vegetation, a mangrove vegetation index has been successfully introduced by Alvin et al. (Alvin et al., 2020) where the authors have successfully demonstrated how to distinguish mangrove spectra from the terrestrial vegetation spectra using sentinel-2 data. The study concludes that terrestrial vegetation has higher reflectance SWIR bands. Sentinel-2 images are suitable for monitoring mangrove regions as they have a good spatial resolution, and the bands in the visible regions, NIR as well as SWIR (Alvin et al., 2020, Prakash et al., 2021). Species scale mapping of mangrove species is done using the help of existing literature data and field trips done on different years. With the help of indices such as NDVI, we can make sense of the overall health of vegetation.

2.6 Spectral data collection

In RS, ground truth refers to at-surface or near-surface observations. The term refers to 'what is actually on the ground that needs to be correlated with the corresponding features in the scene'. Ground truth is important in order to relate data to real features and materials on the ground. The collection of ground truth data enables the calibration of RS data and aids in the interpretation and analysis of what is being sensed. For each location, the respective geographical coordinates are noted.

2.6.1 Field data collection

Data collection was done during noon on sunny days with a cloud-free atmosphere, from 11am to 2pm. It is necessary so that the sun is approximately at the nadir position. Data collection required two people, one to operate the ASD and one to handle the PC which records the data collected. Initial step is the white plate

calibration of the spectroradiometer which is done by a Spectralon plate which gives a reflectance value of one. Once the calibration is done, the optic fiber mounted on a gun is pointed at the object on which to find the reflectance spectra of, without changing the orientation of the gun. Whenever the orientation was changed, or the spectroradiometer was turned off, white plate calibration had to be done again.

2.6.2 Laboratory data collection

For laboratory data collection, a dark room along with a black cloth as background to place the samples are set up. For illumination, a halogen lamp is used as a light source, which is mounted on the tripod and placed such that it emits light in near nadir position. Another tripod is used to mount the data collecting gun placed perpendicular to the field of view. Here one person can perform the data collection, in a controlled environment. (Arun et al., 2015)

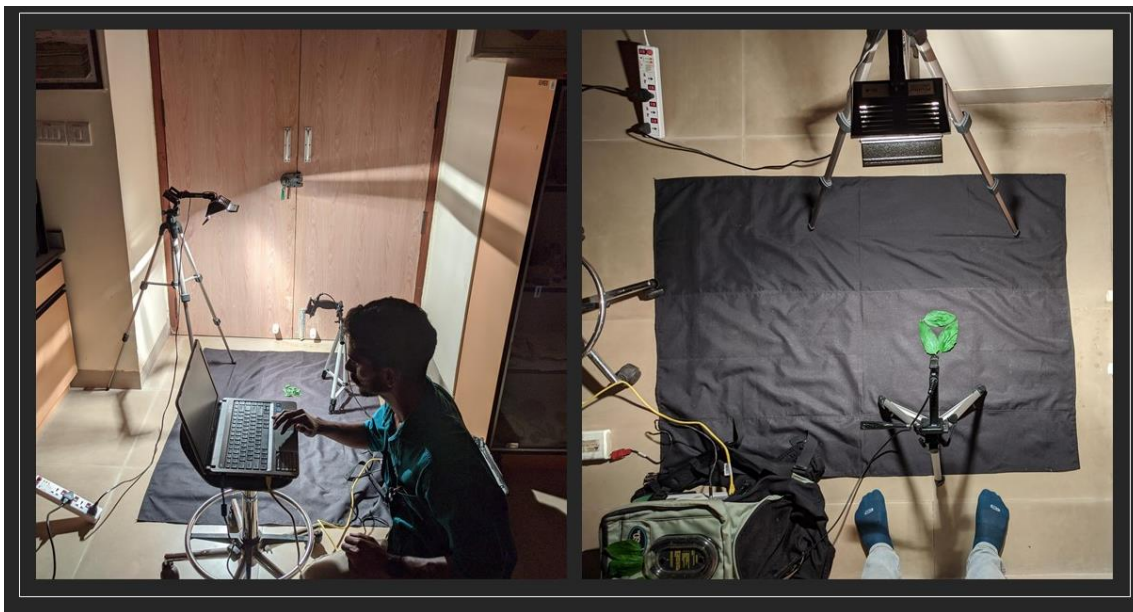


Figure 2.2. Laboratory ASD data collection setup.

2.7 Spectral data Post-processing

Field and Laboratory spectral data post-processing procedures are different. The main difference being the presence of water absorption bands in the field setting and presence of unilluminated wavelength in the laboratory setting.

2.7.1 Drift correction or splice correction

The spectroradiometer used for hyperspectral data collection has three sensors. One 512 channel silicon photodiode collecting spectra in the 350 - 1000 nm region and other two sensors collecting data in the SWIR range (1000 - 2500 nm). The sensors meet at wavelength regions of 1000 nm and 1830 nm (ASD 2010). Due to the inherent property of the sensors, prior to data collection the sensors need to be warmed up, but due to practical difficulty in this process we avoid them. These temperature driven drifts are corrected at the sensor break points of 1001 and 1831 nm by inbuilt splice correction tool in ASD ViewSpec pro software. (Arun et al., 2015)

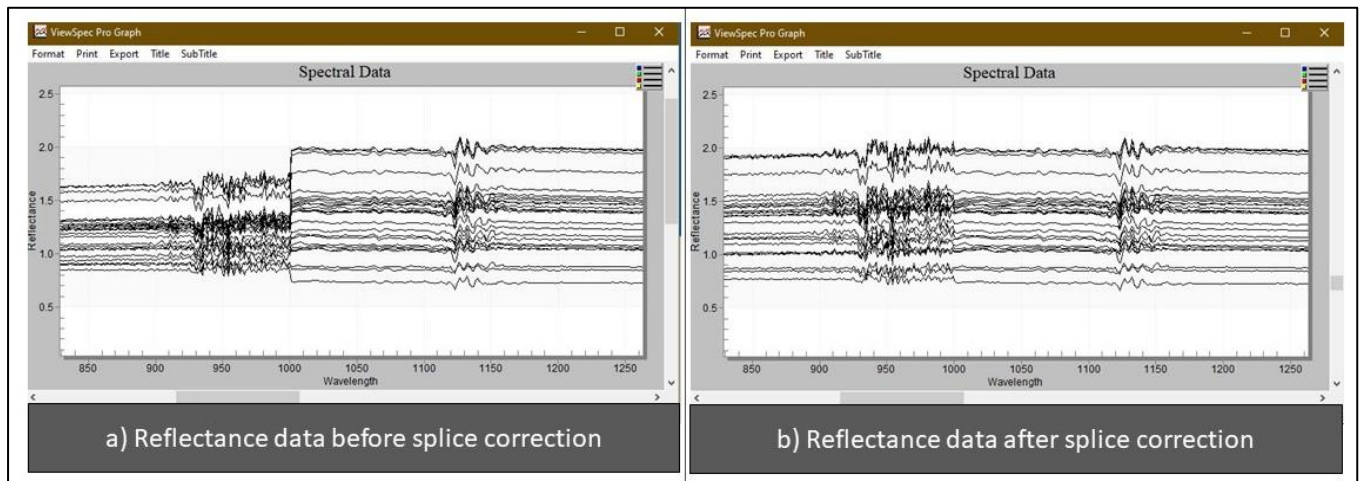


Figure 2.3. Enhanced view of reflectance data at 1001 nm to demonstrate the change in reflectance spectra before and after splice correction.

2.7.2 Removal of water absorption bands and unilluminated bands

There are few bands in the field setting that absorb the EMR radiation in the atmosphere. These are due to the water vapor present in the atmosphere. These regions are represented by vertical strips in the reflectance spectra. During post processing these strips are removed. The wavelength regions that have vertical stripes include 1350 - 1460 nm, 1790 - 1960 nm and 2350 - 2500 nm. These regions come under absorption bands. (Arun et al., 2015)

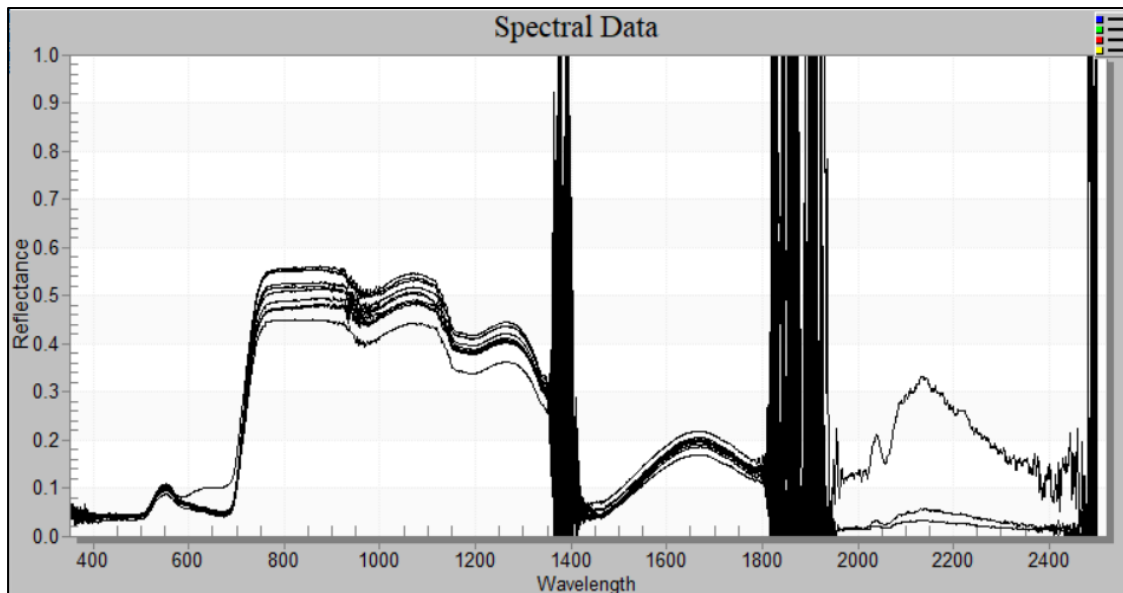


Figure 2.4. Typical field setting ASD spectral data demonstrating atmospheric window region and the absorption band region of electromagnetic spectrum.

In the laboratory setting the source of illumination is halogen lamp which emits radiation from 400 nm to 2500 nm. Hence the data from 350 - 400 nm is removed.

2.7.3 Smoothing of reflectance spectra.

The reflectance data obtained from spectroradiometer have to be smoothed to remove the noise inherent in the sensor due to little energy detected in the narrow bandwidth of hyperspectral sensor (Arun et al., 2015). For the smoothing purpose Savitzky-Golay filter is used through python programming language. It could be seen from figure 2.4 which shows the raw unsmoothed spectra the importance of smoothing the spectra. For both field and lab setting spectra smoothing is done.

2.7.4 Resampling hyperspectral data to Sentinel 2 spectral resolution

This was done using the python programming language. The central wavelength and bandwidth of Sentinel 2 was considered from table 1 and using that as reference, the hyperspectral data was resampled to Sentinel 2 band resolution.

2.8 Ground Truths (GTs) data collection

GT data was collected by field visits and also from the existing literature on the study sites. Field data collection in the East coast was done in 2013. Along with reporting the species of mangroves present in a particular location, spectral reflectance data was also collected and a spectral library of mangrove species was made, which was provided for this study. Along the west coastline, field data was collected in 2019 and in 2022. 2019 data was provided for study purpose, and I was part of field data collection done in 2022. Transect surveys were conducted as part of fieldwork. The transects were selected according to ease of access and opinion from forest officers and local people. Along the transects, species diversity was documented at 15 m spacing. As mangroves exist along the intertidal zones, data collection was effortful. The strategy was to start from the accessible area near to the creek and move landwards collecting spectral data. In figure 2.5 one of such field survey transect is shown mentioning the accessible area near to the creek. The data collection was done during low tide time in the area.



Figure 2.5. GT points and transect survey done for Thane region. (Survey transect is shown in red line).

Chapter 3 Results and Discussion

3.1 Reflectance spectra collected by onsite field visits

Reflectance spectra of matured leaf of mangrove species is shown in figure 3.1.1. Since reflectance spectra depends on the phenological stages of plant, only spectra data from matured leaves was taken. For the West coast, the reflectance data shown is the average of 10 – 15 samples, with each samples taking 25 instances of spectra. There is variation in the field spectra and laboratory spectra of west coast in terms of range of reflectance values or the mangrove species, this is due to the fact that few samples were considered for taking the average spectra. While for the east coast, the spectral library was made by averaging the ASD hyperspectral data of around 100 samples. Hence the data seems to be reliable for studies done using reflectance spectra as a reference spectrum such as in the spectral angle mapper algorithm, applied to airborne satellite data providing highly accurate results.

Compared to east coast spectra west coast mangroves species have considerably lower reflectance values. It could be an inherent property or dissimilarity among the species present in the two coasts. Figure 3.1.2 and 3.1.3 gives a comparison between resampled hyperspectral data to Sentinel 2 resolution and the image spectra from different study sites (for Sentinel 2 image spectra for different study sites, the reflectance values given are upscaled by 10,000). For the west coast region, the image spectra and resampled field spectra does not agree with each other. In both Sadamirya and Malad region higher reflectance is seen for *Rhizophora sp* but the field data implies *Rhizophora sp* has lowest reflectance curve among the species considered. This could not be validated as the field data obtained is having fewer sample size. East coast image spectra and resampled field spectra of East coast have comparably better correlation.

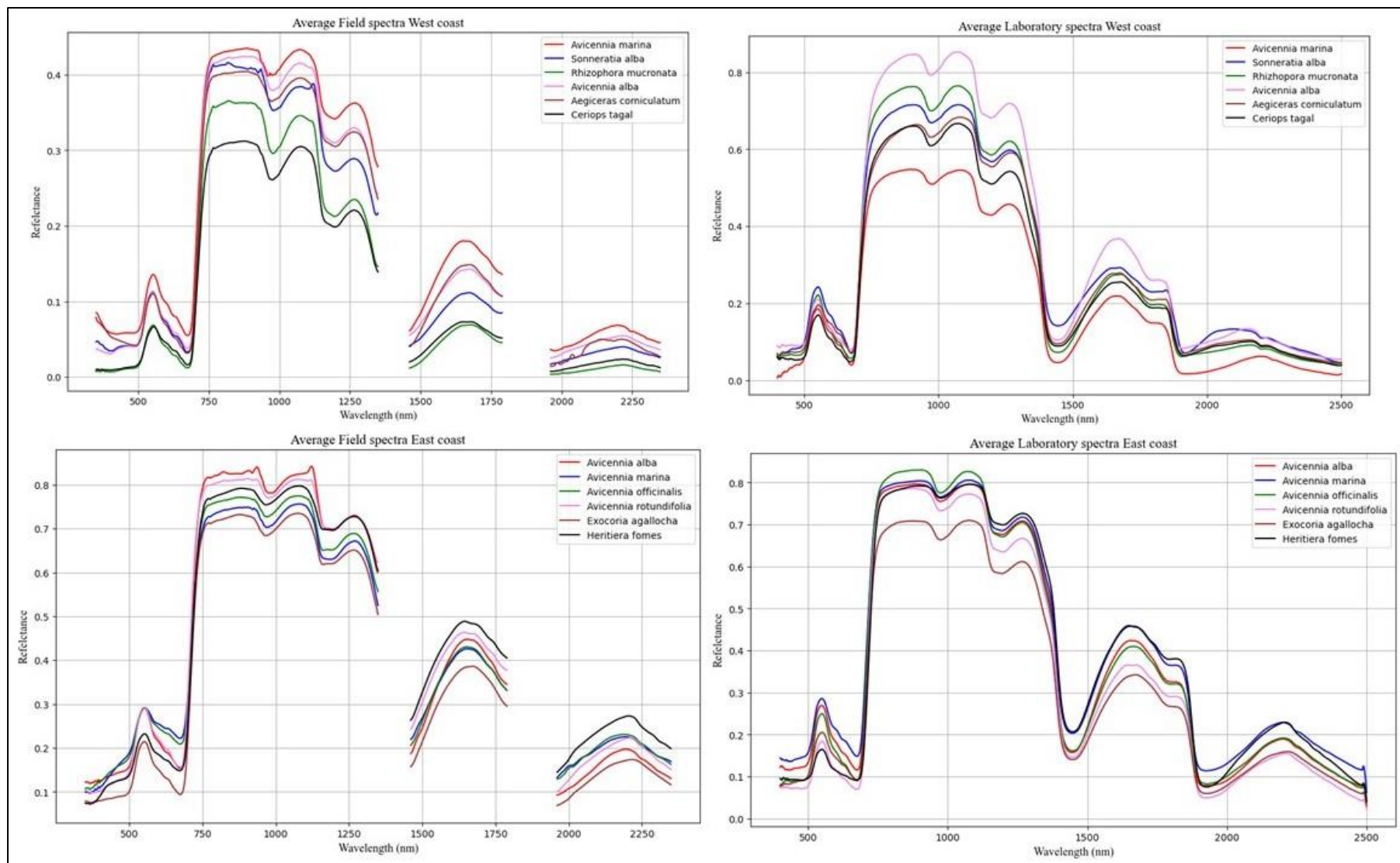


Figure 3.1.1 Reflectance spectra collected from field surveys. Post processed hyperspectral data is shown in the figure.

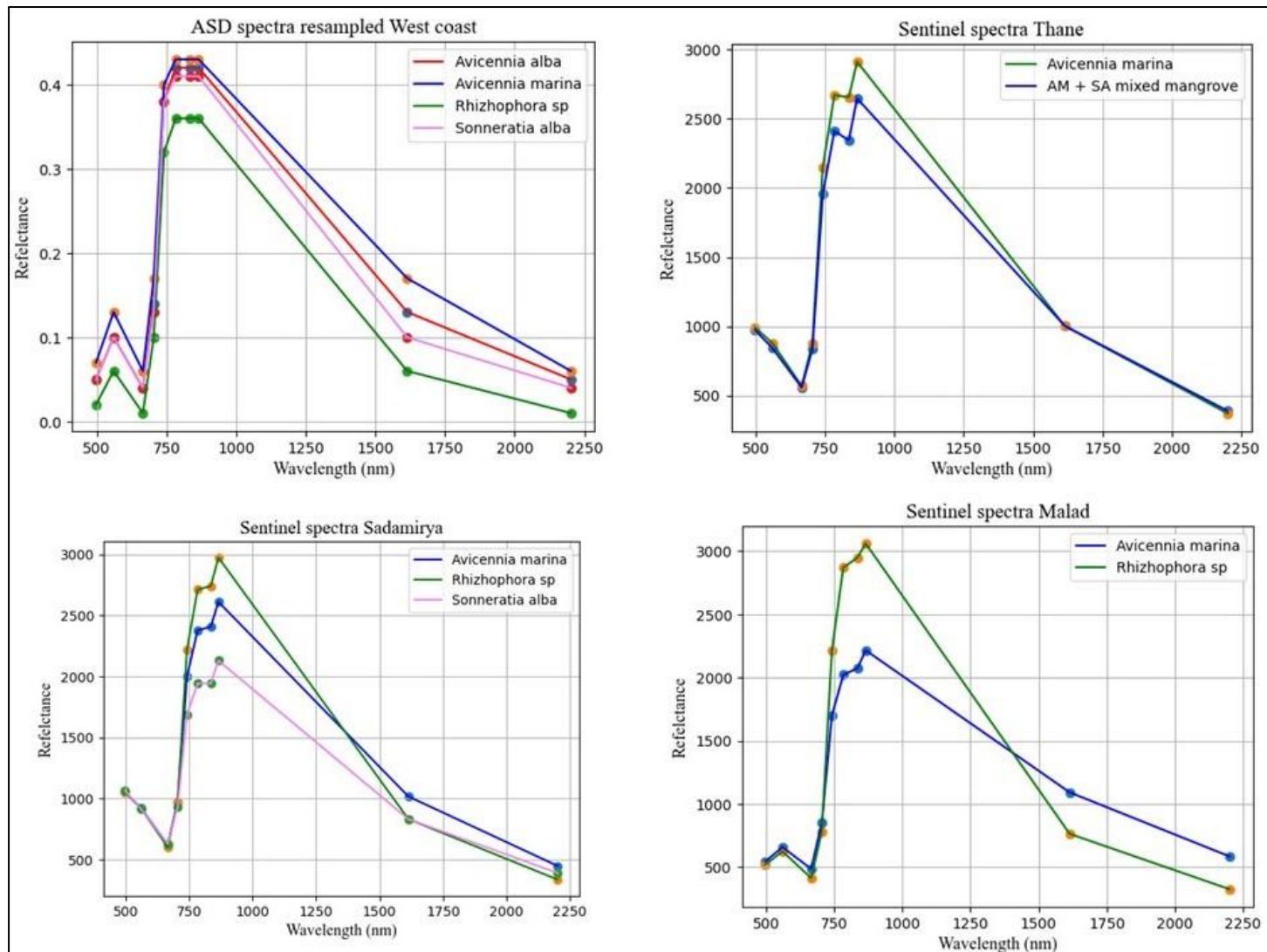


Figure 3.1.2 West coast ASD reflectance data resampled to Sentinel 2 resolution and compared to study sites along west coast. (for thane region the legends are different than other images.)

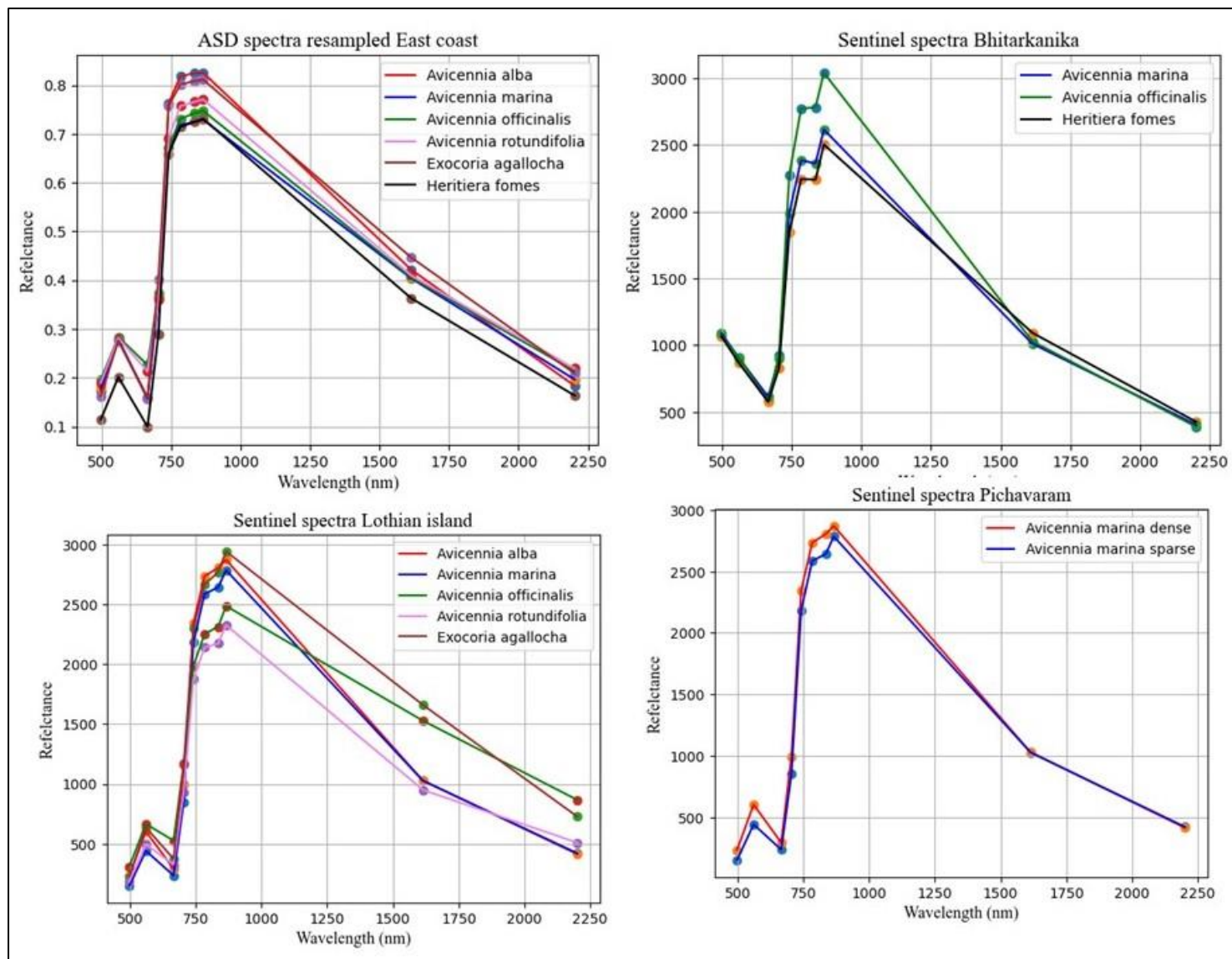


Figure 3.1.3 East coast ASD reflectance data resampled to Sentinel 2 resolution and compared to study sites along east coast.

Table 3.1. Species identified in different study sites and the source of data.

Study Site	Species Identified	Literature data	Field Data	Sentinel 2 MGRS tile	EPSG (CRS)
Thane creek	AM SA		Yes	43QBB	32643
Sadamirya	SA AM RH	Mulla et al, 2017	Yes	43QCU	32643
Bhitarkanika	HF AO AM MX1 - AO+EA MX2 - AO+EA+HF	Padma et al., 2014 Hati et al., 2021	Yes	45QVC	32645
Lothian Island	AM AA AO AR EA MX1 - AR+AM+CD MX2 - PP+AM+EA	Hati et al., 2021 Chaube et al., 2019	No	45QXE	32645
Pichavaram	RH AM	Gnanappazham & Selvam, 2014 Kripa et al. 2019	No	44PLT	32644
Malad	RH AM	Nagarajan, et al.,2022	Yes	42QZG	32643

As seen from figures 3.1.2 and 3.1.3, the sentinel image spectra distinguishes mangrove species in the bands: Band 6, Band 7, Band 8, Band 8A (RE4) and Band 11. These corresponds to wavelength region of Red Edge (RE), NIR and SWIR. Although species have significant difference in reflectance spectra in the green domain of spectrum, it is evident only in the Level 2A images. For time series analyses the time series trend in the bands which discriminate between species is considered.

3.2 Thane

With an area of 49.56 km², Thane region is one of the biggest region where the study is carried out. This region is along the west coast and is dominated by *Avicennia marina* (AM) mangrove species. From figure 3.2.1, the band combination of Agriculture shows brighter shades of green in the region adjacent to the creek. This could be a different species of vegetation, but with onsite visits it indicates that these are matured, bigger crowned trees of AM. The size of tree crown size gets smaller towards inland. The spectral separability analysis of different ROIs indicated good separability (figure 3.2.3). The classification accuracy is >0.96 for both the initial and final classification images (figure 3.2.2).

Towards the north part of the study site there are pockets of *Sonneratia alba* (SA) present, in between *Avicennia marina* species. These regions are mapped as mixed species in the classification output. These mixed patches have increased in area (0.97 km²) in the study span while AM have decreased by 3.03 km². From figure 3.2.2, the region mapped as AM in 2015 November image has converted to mudflats in the southern part of the study region. The time series plot for different bands, figure 3.2.3 shows the decrease in reflectance values for RE and NIR regions. While for SWIR band, the reflectance trend have shown a peak in the year 2020 November image, indicating a poor health of species.

The yearly NDVI analyses shows a drastic decrease in vegetation health from the year 2018 as shown in figure 3.2.4, and from 2020 the vegetation is showing gradual recovery from stressed condition. Although the north part of study area gradually seems to be recovering from stressed condition, the southern part of the study area, as shown in the figure 3.2.2 where AM stands have degraded, have converted to mudflats. The seasonal NDVI analysis, figure 3.2.5 shows the better health of mixed mangrove class across years. From the initial year of 2016, the NDVI trend shows a downhill pattern. Apart from the general conclusion, there is no cyclical pattern of healthier month for vegetation observed.

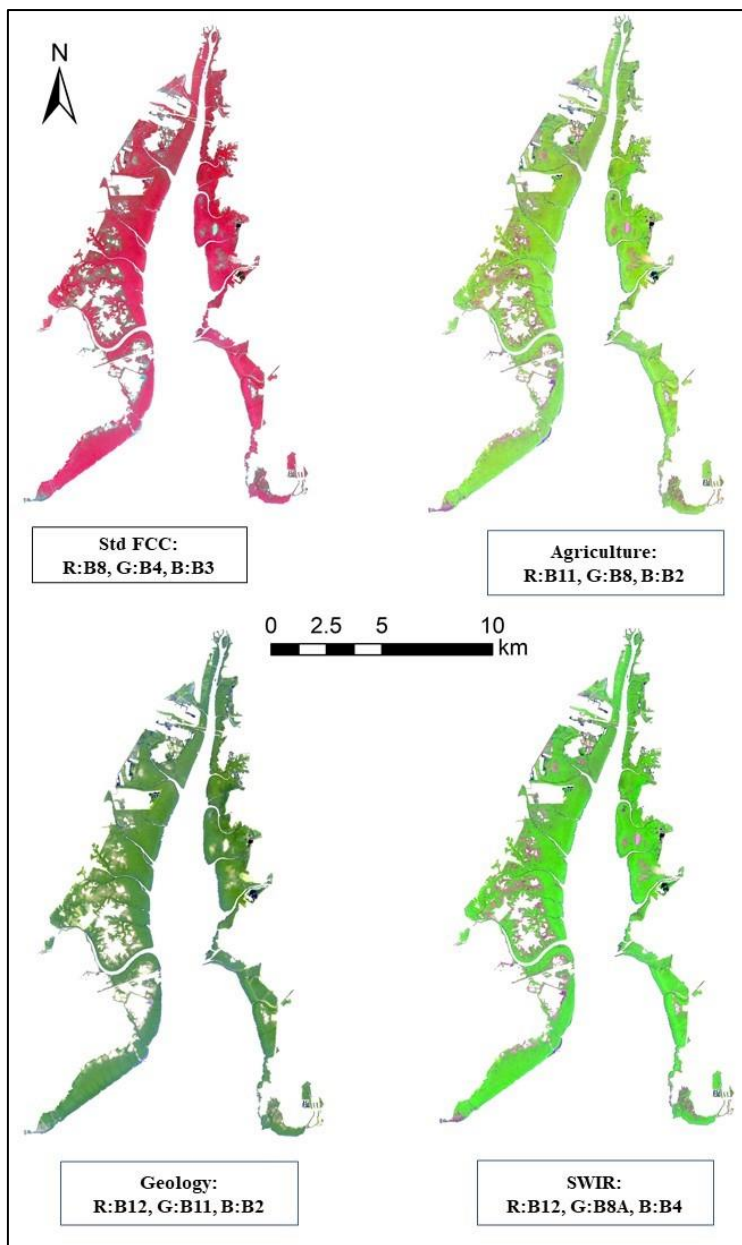


Figure 3.2.1 Color composites of Thane study.

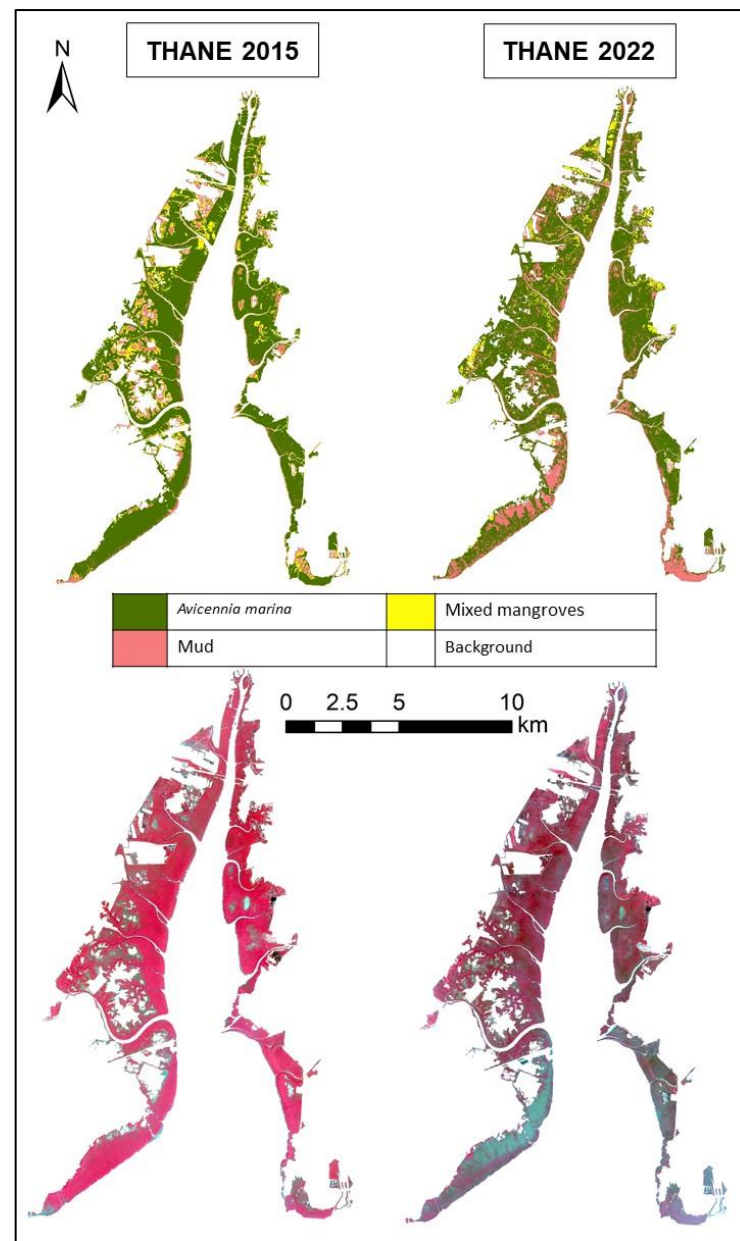


Figure 3.2.2 Classification outputs for Thane site.

Table 3.2.1 Land cover of different mangrove species: Thane region.

	Initial area (km ²)	Final area (km ²)
Mud	4.26	7.75
<i>Avicennia marina</i>	37.65	34.62
Mixed mangroves	6.07	7.04

Table 3.2.2. Accuracy assessment for Thane region.

Random Forest classifier	Overall accuracy	Kappa coefficient
Initial image (Nov 2015)	0.99	0.98
Final image (Nov 2022)	0.97	0.96

Table 3.2.3 JM distance matrix for Thane.

	AM	MX	Mud
AM	-	1.98	2
MX	1.98	-	2
Mud	2	2	-

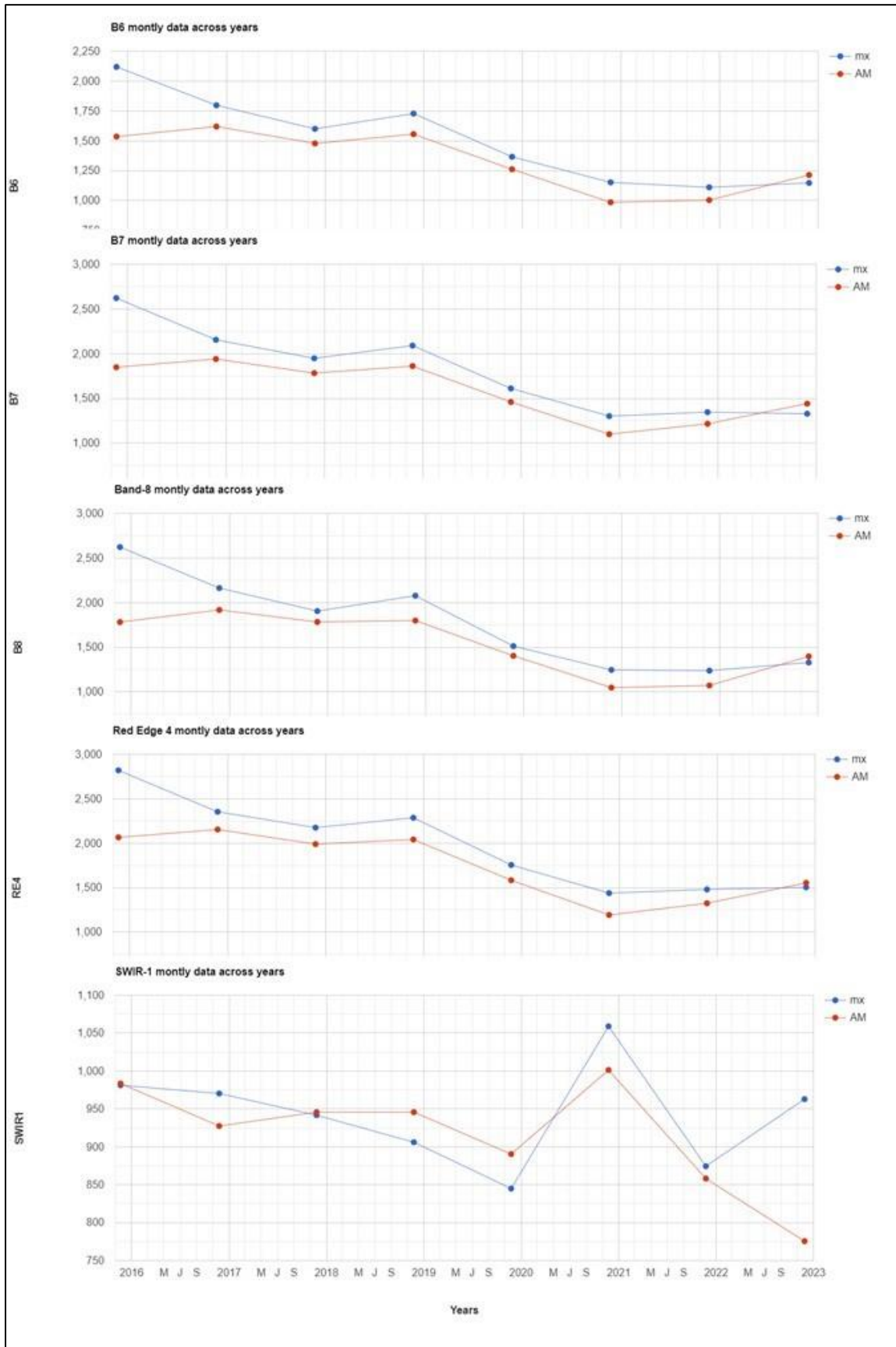


Figure 3.2.3 Yearly data for November 2015 - 2022 for Band 6, Band 7, Band 8, Band 8A (RE4) and Band 11 for Thane.

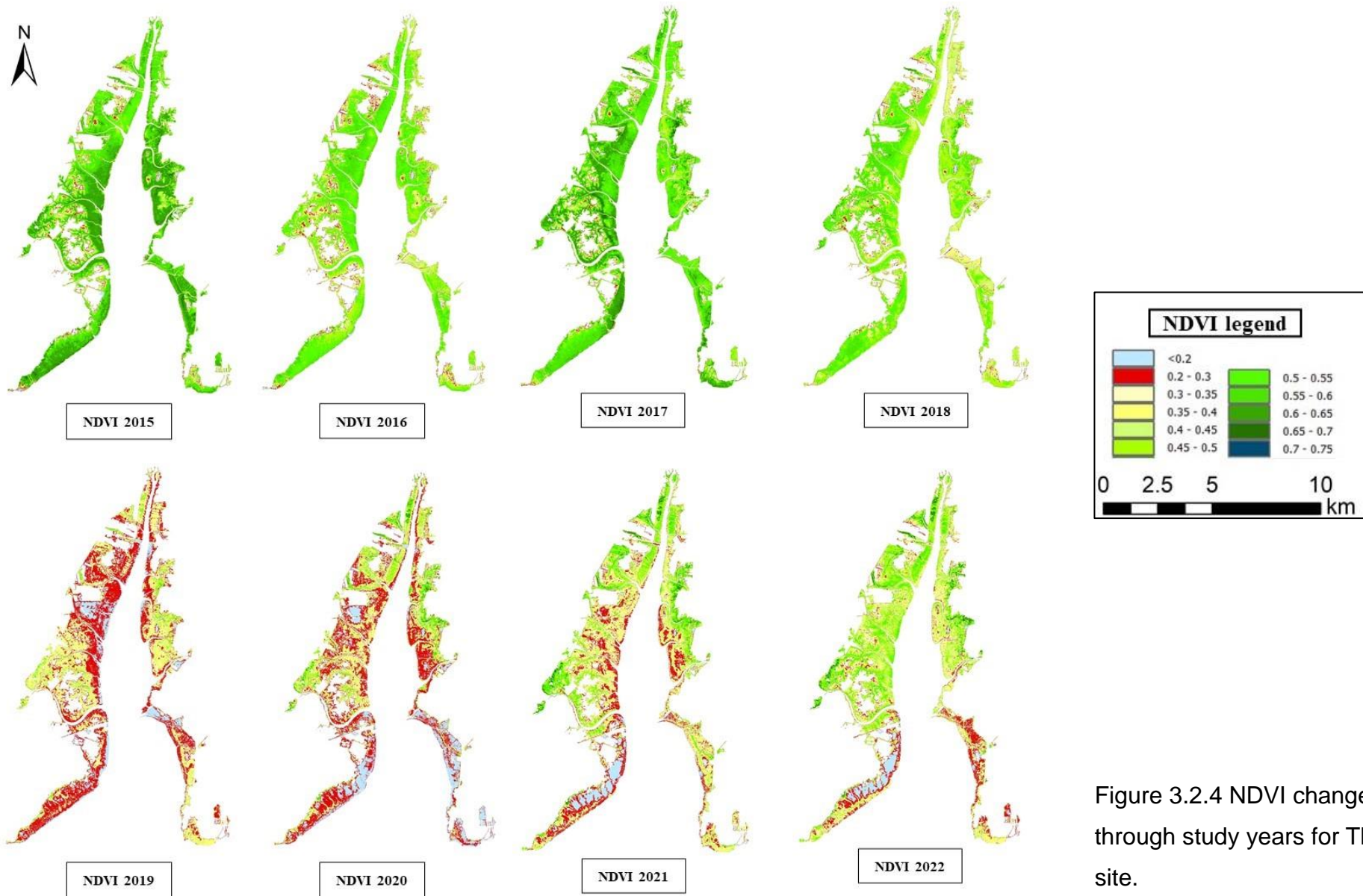


Figure 3.2.4 NDVI changes through study years for Thane site.

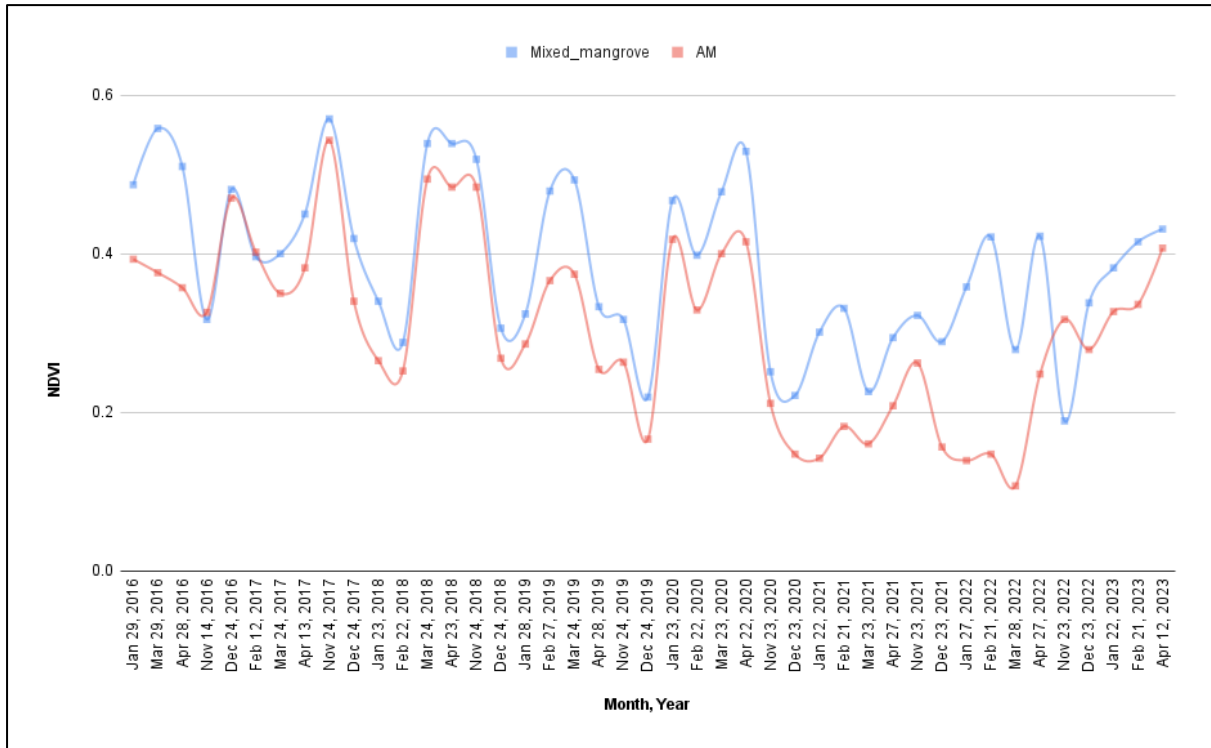


Figure 3.2.5. NDVI seasonal trend from 2016 – 2023 for the two mangrove classes in Thane region.

3.3 Sadamirya

Sadamirya study site is along the west coast having an area of total 3.61 km². The region is dominated by *Sonneratia alba* (SA) and *Avicennia marina* (AM) species. Preliminary analysis shows the color variations in the Agriculture and SWIR band combinations, where there are two shades of green color. The brighter green and the darker shade of green. Since the brighter green shade is present in towards the land and the other towards the creek side, this hinted towards the possibility of different mangrove species. It was identified that there exist some patches of *Rhizophora sp.* (RH) in the area.

Accuracy assessment (table 3.3.1) and JM separability matrices (table 3.3.2) shows reliable results. From figure 3.3.4, there are no apparent changes in the band trend for the species ROIs across years. From figure 3.3.2, the classification output along with data from table 3.3.3 indicated the increase in area of distribution of RH and terrestrial vegetation (TV). While AM stands have slightly increased in area, SA have decreased and it is occupied by AM as observed from classification output.

The yearly NDVI analyses for the month of November shows a cyclical trend as the patches of vegetation classified as SA experiences stress (figure 3.3.3).

The seasonal NDVI analysis, figure 3.3.5 shows the better health for RH followed by AM and SA. The yearly data shows that from the data taken, the months of November – December shows the healthier vegetation.

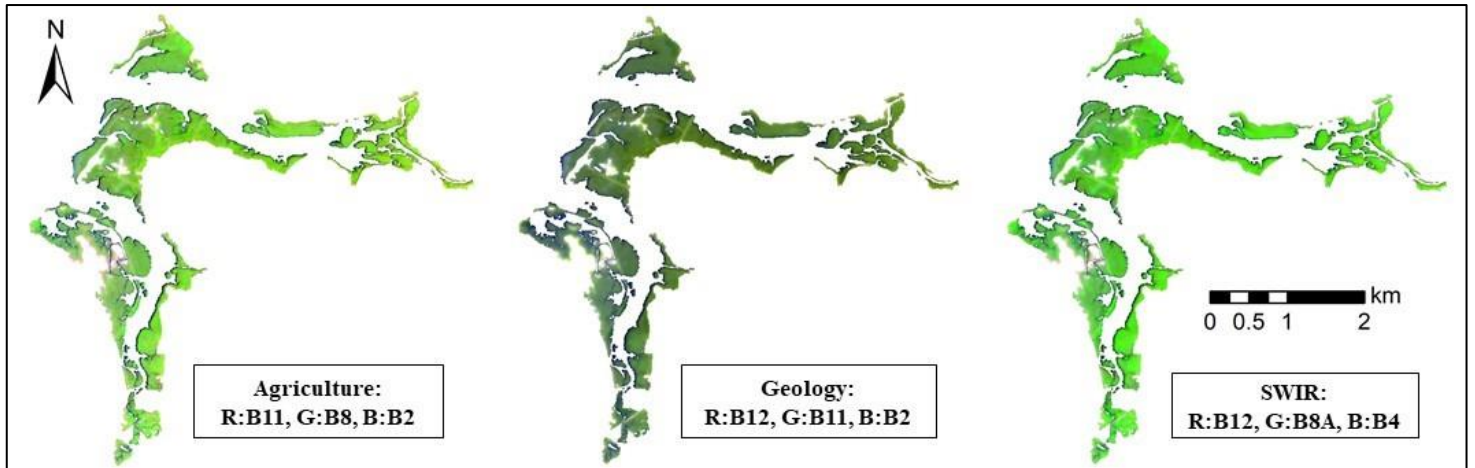


Figure 3.3.1. Different band combinations for Sadamirya study site.

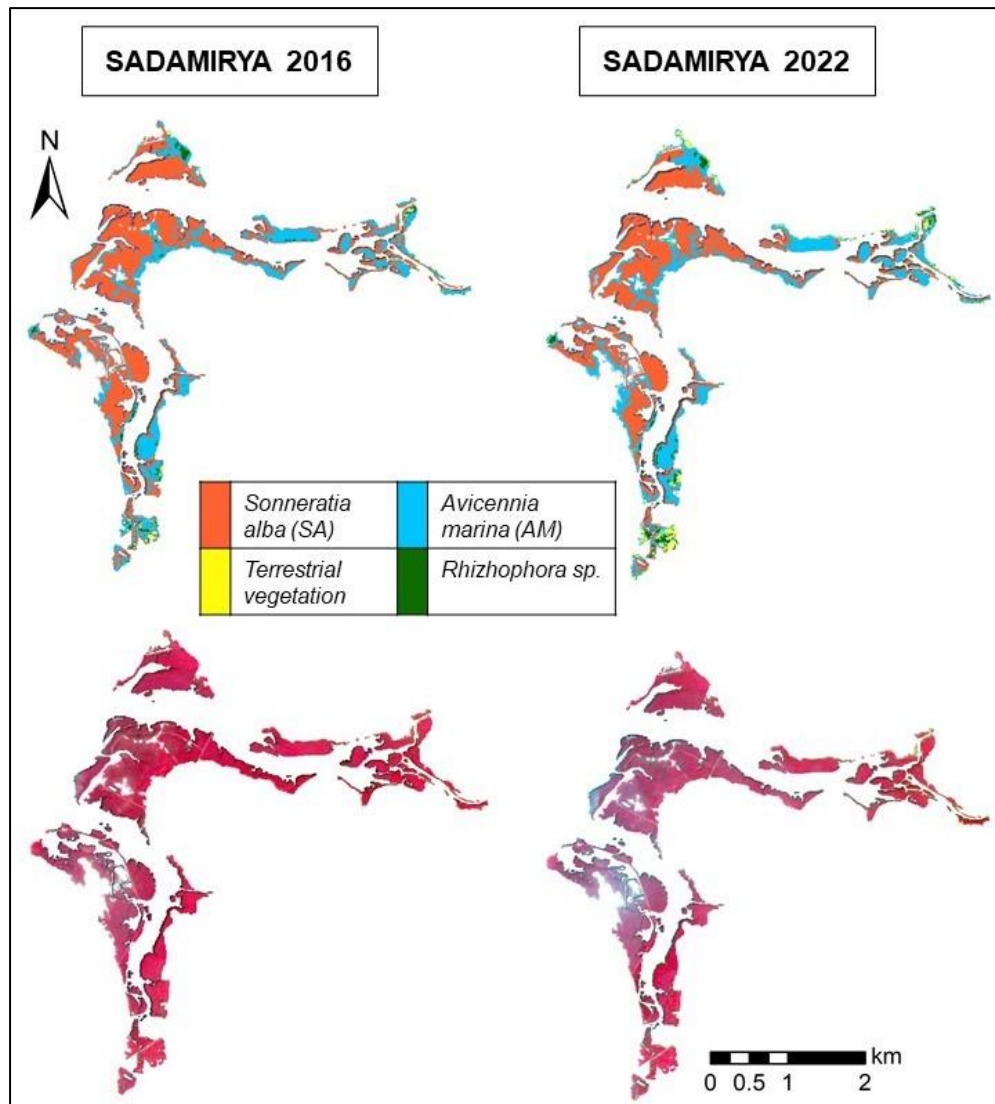


Figure 3.3.2 Classification output for Sadamirya site.

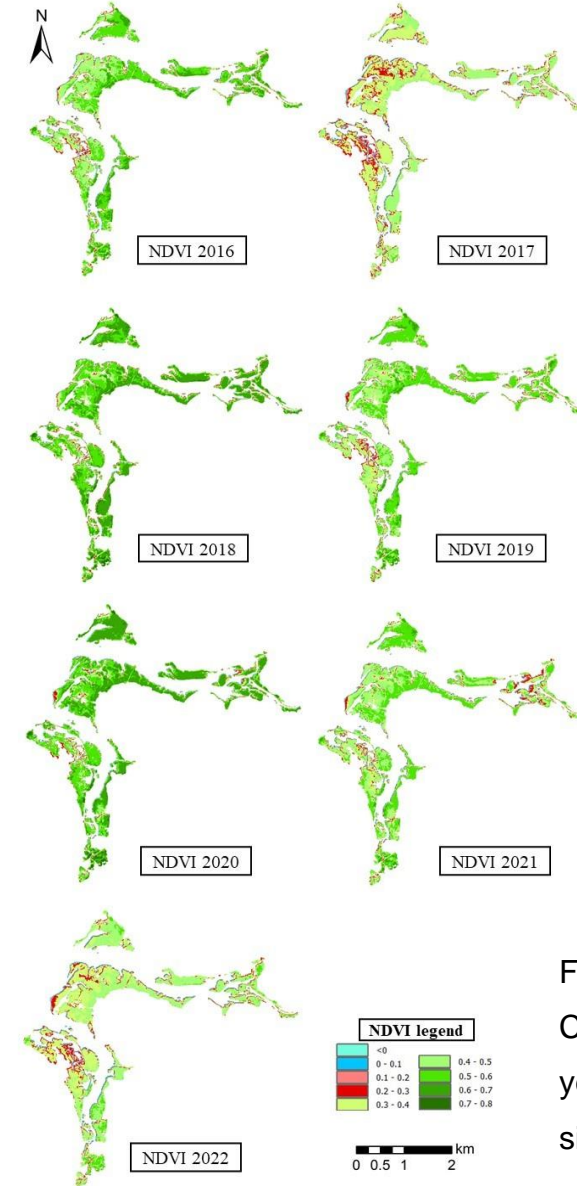


Figure 3.3.3 NDVI Changes through years for Sadamirya site.

Table 3.3.1 Accuracy assessment: Sadamirya region

Random Forest classifier	Overall accuracy	Kappa coefficient
Initial image (Nov 2016)	0.99	0.98
Final image (Nov 2022)	0.98	0.97

Table 3.3.2. JM distance matrix for Sadamirya.

	RH	AM	SA	TV
RH	–	1.93	1.99	1.88
AM	1.93	–	1.92	1.94
SA	1.99	1.92	–	1.99
TV	1.88	1.94	1.99	–

Table 3.3.3 Land cover of different mangrove species: Sadamirya region

	Initial area (m ²)	Final area (m ²)
<i>Rhizophora sp.</i>	89,149.96	98,315.73
<i>Avicennia marina</i>	11,10,606.28	11,06,357.76
<i>Sonneratia alba</i>	18,67,122.23	16,73,712.72
Terrestrial vegetation	35,183.89	1,96,203.58
Mud	4,97,796.45	4,95,269.03

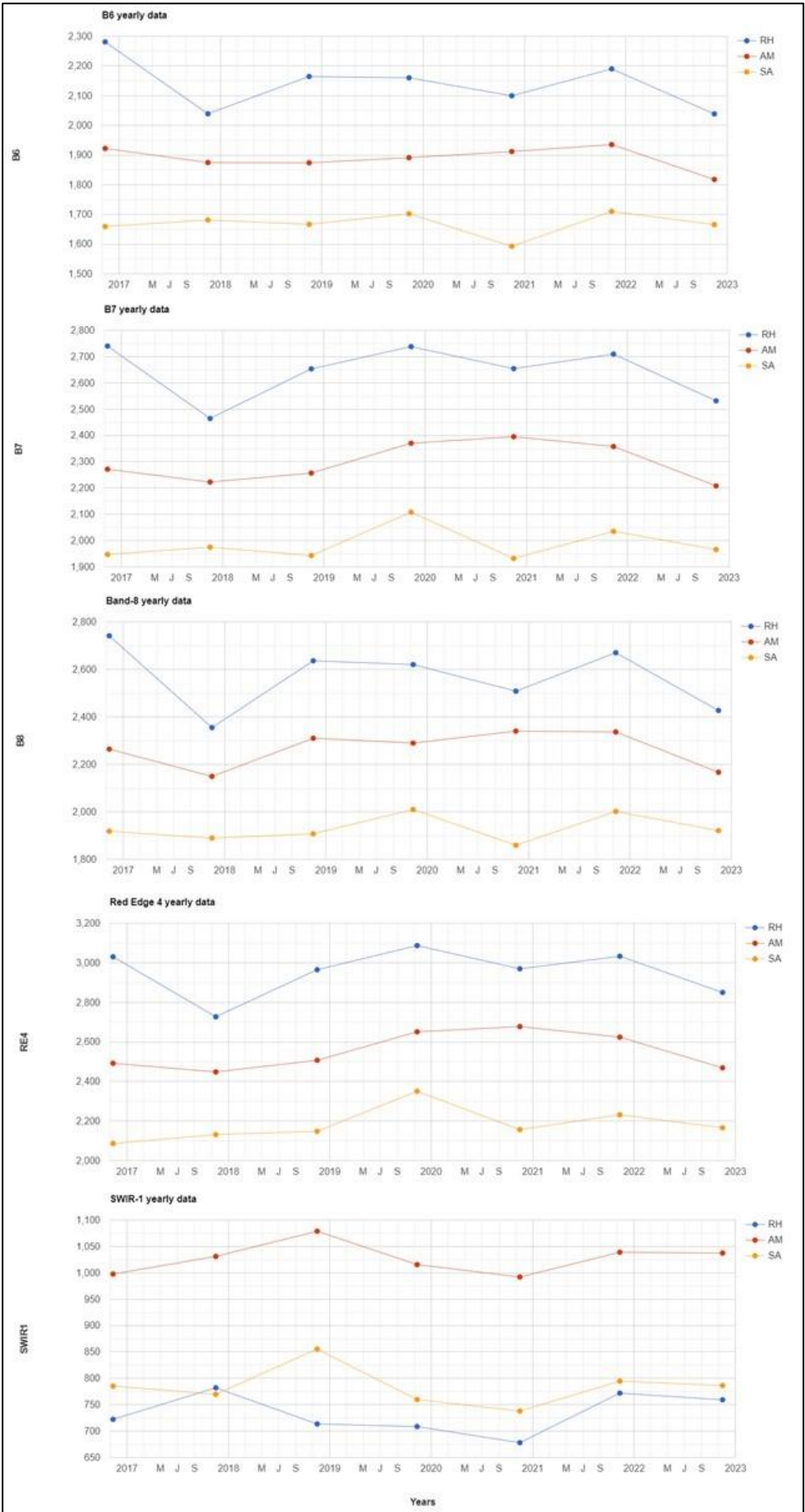


Figure 3.3.4. Yearly data for November 2016 - 2022 for Band 6, Band 7, Band 8, Band 8A, Band 11 for Sadamiya.

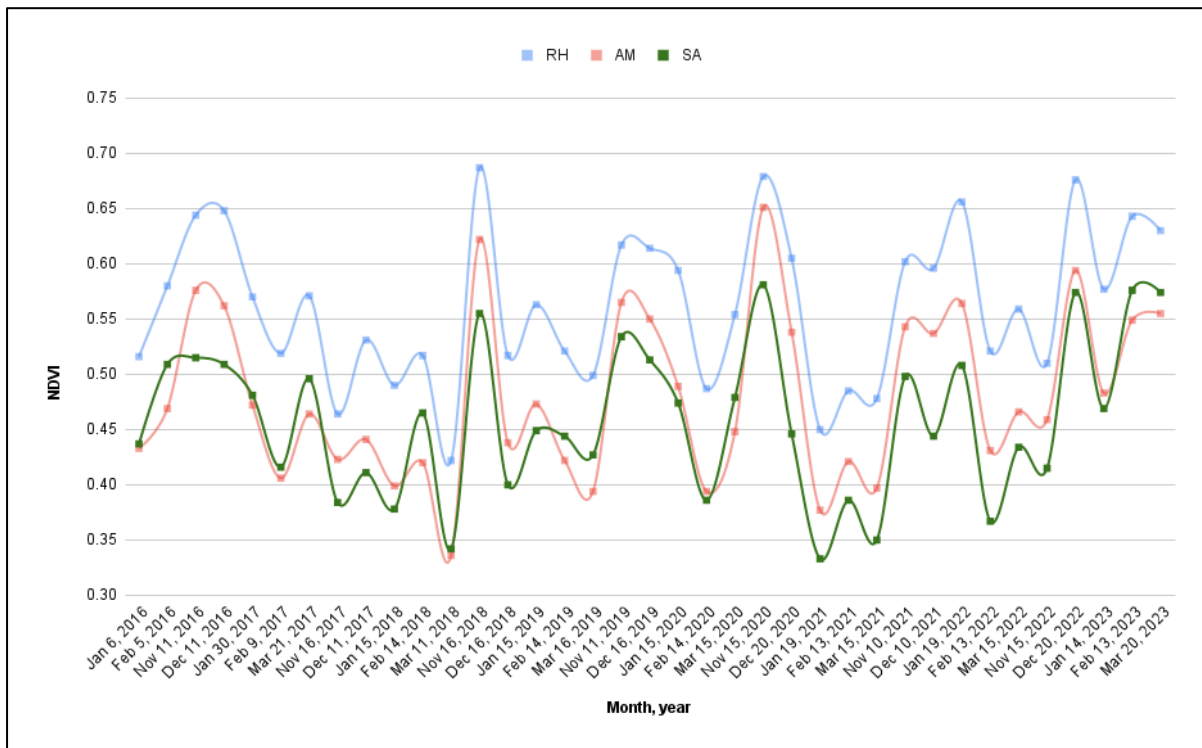


Figure 3.3.5. NDVI seasonal trend from 2016 – 2023 for each species of Sadamirya.

3.4 Bhitarkanika

Study area for Bhitarkanika is 48.28 km². This region is in the East coast of India, and the dominant mangrove species found here include *Heritiera fomes* (HF), *Excoecaria agallocha* (EA), and *Avicennia officinalis* (AO). Figure 3.4.1, the preliminary analysis showed hints of multiple species as the color composites showed different shades. There was one prominent strip, found out to be terrestrial vegetation that ran across the study area in the middle of core mangroves. The different shades of orange and green from color composite agriculture indicates different species of mangrove vegetation.

From the classification output it was evident that the HF has grown in the sparse population to dense, also it was evident that AO has grown and spread to new areas between 2016 and 2022 (figure 3.4.2). This is supported by the band time series as towards the year 2022 the reflectance values were higher for all RE and NIR bands for AO and HF (figure 3.4.3). The change in area as reported from the classification images and described in table 3.4.3 shows that AO have increased in area from 5.11 km² to 7.58 km². The mangrove class HF has spread into the sparse regions and increased in area by 2.17 km². The decrease in area of HF sparse is around 52.2% and this area is occupied combinedly by HF dense and mixed species (MX1) of

Excoecaria agallocha (EA) and *Avicennia officinalis* (AO), where the MX1 class has increased in area by 1.36 km². Rest of the classes such as AM, Terrestrial vegetation (TV), Mixed class 2 (MX2), and mud have slighter variations in areal change in comparison. (MX2 : AO+EA+HF mixed).

Separability analysis of the spectra collected from Sentinel 2 images resulted the JM matrix values to be more than 1.5 for all the major mangrove species, except the lower value of 1.42 between HF dense and HF sparse, i.e., for the same species with density variation.

The seasonal NDVI analysis shows a decreasing trend with time as shown in figure 3.4.5. For any year, vegetation health is at its peak during November – December, but the lack of data during May to October, when the region is covered with cloud hinders further conclusions on the peak health or stressed conditions. The yearly NDVI image figure 3.4.4 used for time series analysis shows that the vegetation was healthier during December 2016, and towards 2022 health is regained after a dip in the previous years.

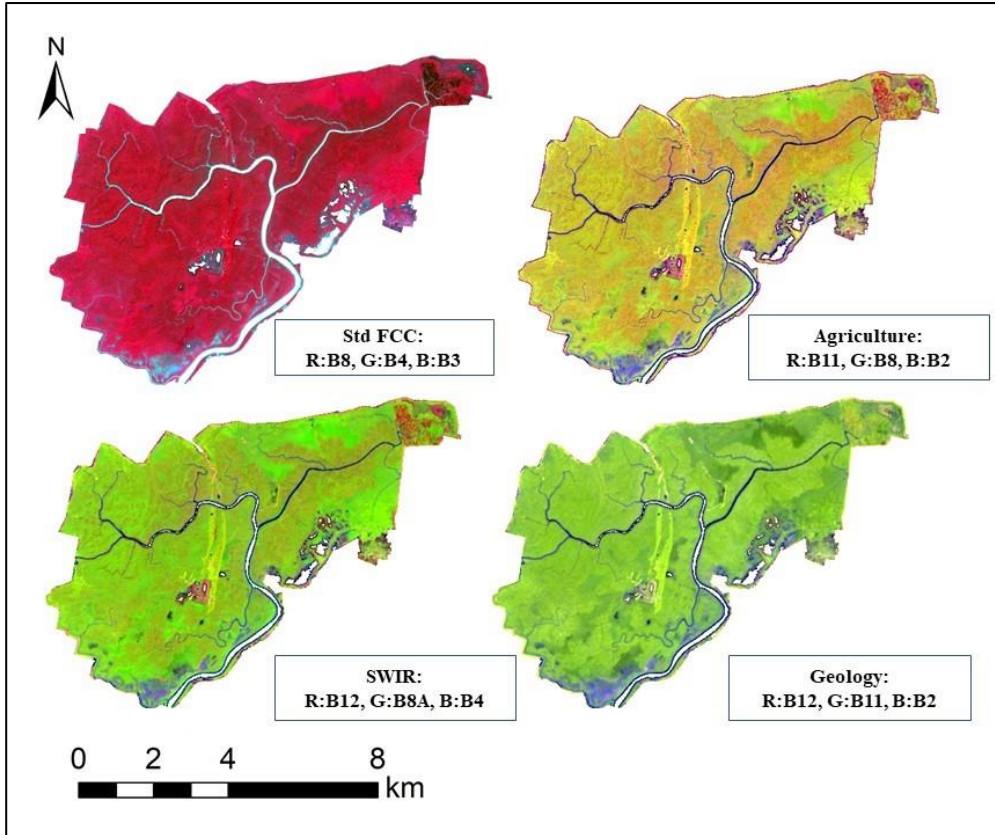


Figure 3.4.1 Color composites of Bhitarkanika study site.

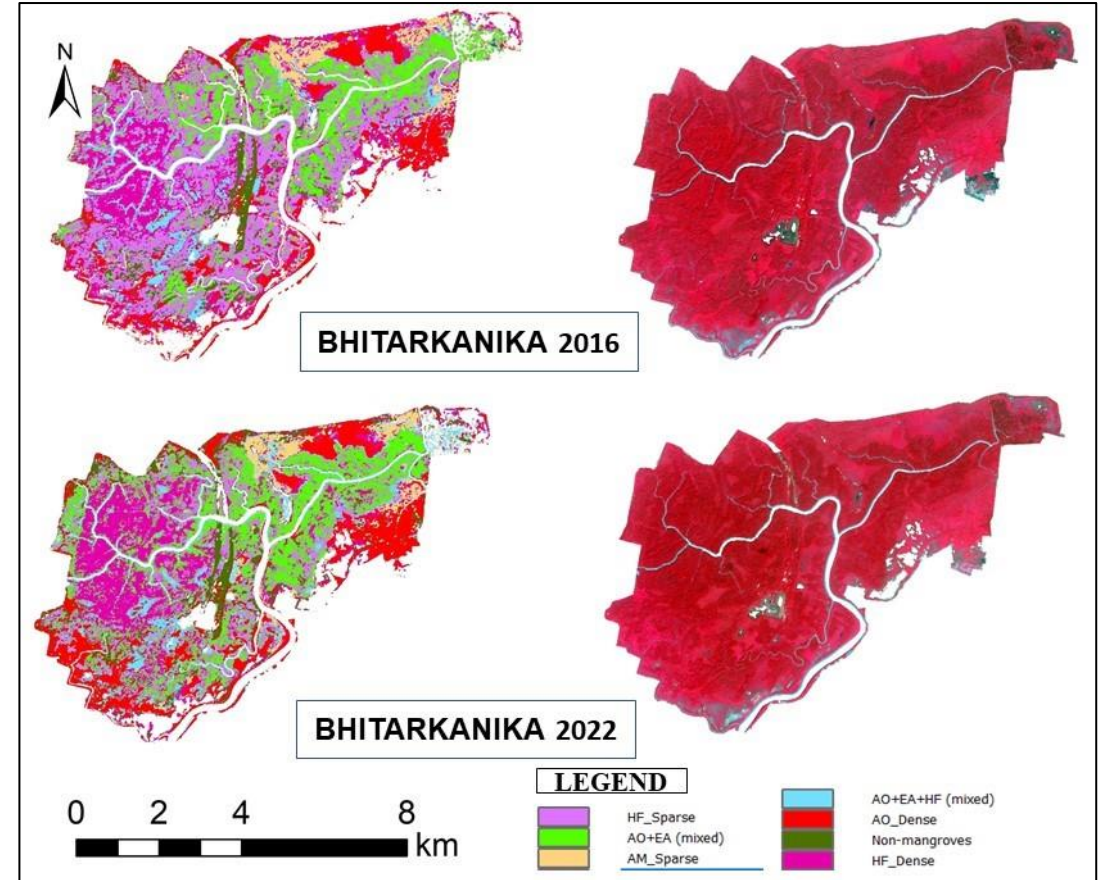


Figure 3.4.2 Classification output using Sentinel-2 L1C product. 2016 December image and 2022 November image considered for classification of the respective years.

Table 3.4.1 Accuracy assessment: Bhitarkanika

Random Forest classifier	Overall accuracy	Kappa coefficient
Initial image (16 th Dec 2016)	0.99	0.99
Final image (16 th Nov 2022)	0.98	0.98

Table 3.4.2 JM distance matrix for Bhitarkanika.

	AO_Dense	NM	HF_dense	HF_sparse	AO+EA (mixed)	AM_sparse	AO+EA+HF (mixed)
AO_Dense	-	1.75	1.80	1.98	1.99	1.97	1.93
NM	1.75	-	1.68	1.83	1.98	1.90	1.83
HF_dense	1.80	1.68	-	1.42	1.94	1.76	1.68
HF_sparse	1.98	1.83	1.42	-	1.64	1.98	1.96
AO+EA (mixed)	1.99	1.98	1.94	1.64	-	1.99	1.99
AM_sparse	1.97	1.90	1.76	1.98	1.99	-	1.97
AO+EA+HF (mixed)	1.93	1.83	1.68	1.96	1.99	1.97	-

Table 3.4.3 Land cover of different mangrove species: Bhitarkanika region

	Initial area (km ²)	Final area (km ²)
MUD	4.15	4.85
<i>Avicennia officinalis</i>	6.11	7.58
<i>Heritiera fomes</i> Dense	9.55	11.72
<i>Heritiera fomes</i> Sparse	11.18	5.34
<i>Avicennia marina</i>	2.27	2.25
MX1	7.65	9.01
MX2	3.61	3.92
Terrestrial vegetation	3.76	3.61

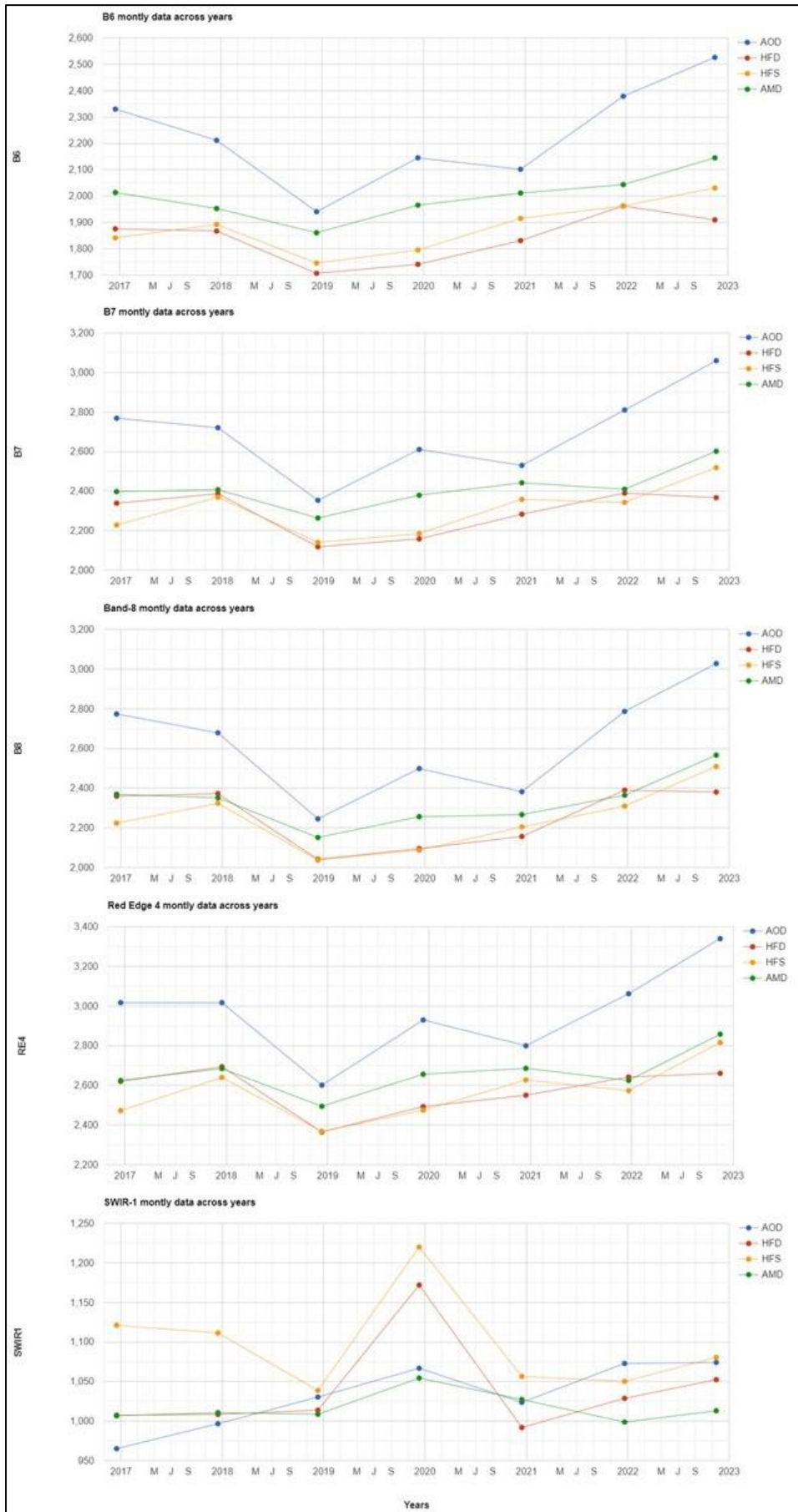


Figure 3.4.3. Yearly December data for Band 6, Band 7, Band 8, Band 8A, Band 11 from 2016 – 2022 for Bhitarkanika.

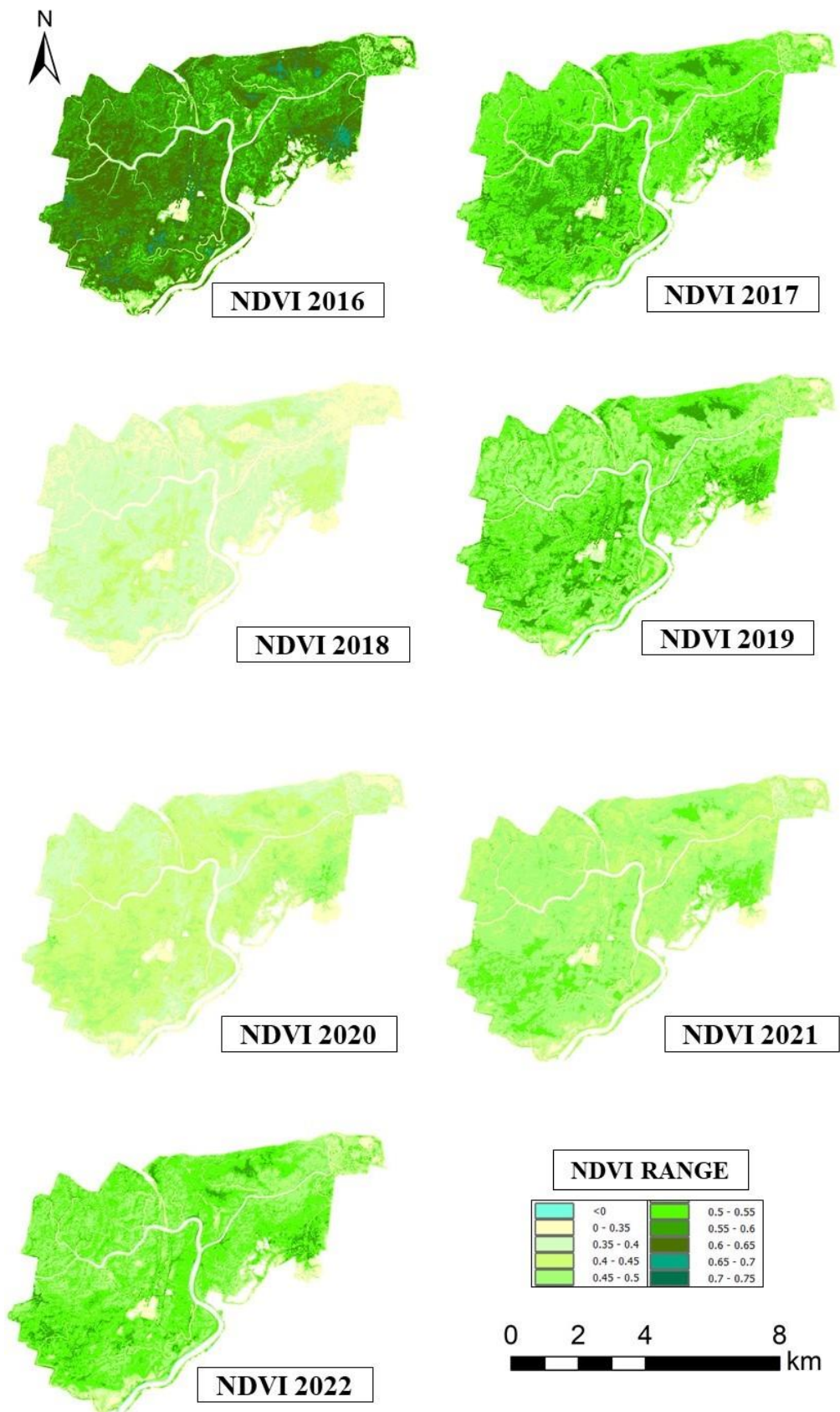


Figure 3.4.4. NDVI image of December 2016 – 2022 with range.

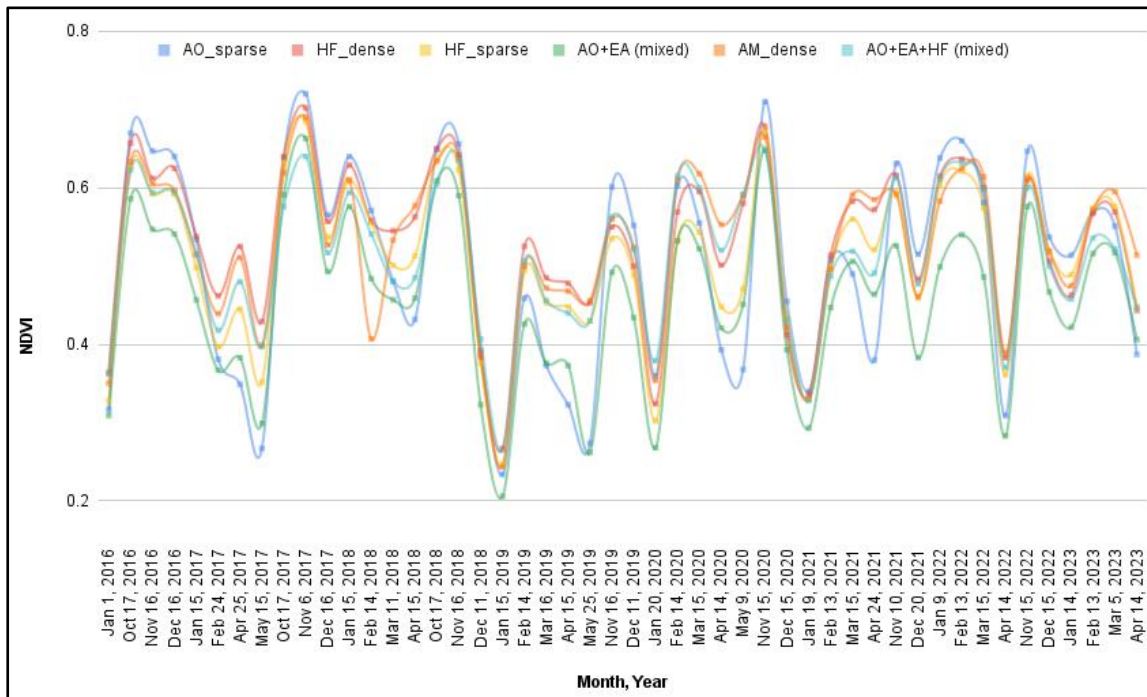


Figure 3.4.5. NDVI seasonal trend from 2016 – 2023 for each species of Bhitarkanika.

3.5 Lothian Island

Lothian Island study site has a area of 34.65 km² of mangrove vegetation. It belongs to the Indian part of Sundarbans and shows diversity in mangrove species with five true mangroves mapped and two mixed mangroves identified using Sentinel 2 imagery. The dominant species mapped include *Avicennia marina* (AM) followed by *Avicennia alba* (AA). Most of the region is covered with mixed mangrove patches, with MX1 consisting of *Aegialitis rotundifolia* (AR), *Avicennia marina* (AM) and *Excorcaria agallocha* (EA). The preliminary analysis, figure 3.5.1, did not yield much information other than the presence of vegetation in bright green patches and degrading sparse vegetation in between the lush patches.

JM separability analysis for the spectra collected for major mangroves and mixed mangroves showed good separability with values to be more than 1.79. The classification output shows some new patches of vegetation in the 2023 February image compared to the 2019 February image (figure 3.5.2). This was further looked into and concluded based on the very high resolution google earth images that there is indeed mangrove growth in the region.

From the classification images in figure 3.5.2, it is observed that there is a shrinking in the area covered by AR, and it has shrunken from 2.05 to 1.62 km² in area. AM species has grown in area by 1.08 km² as depicted in table 3.5.3. AA, AO and MX1 have increased in area while EA, MX2 have decreased. (MX2 : Phoenix paludosa (PP) + AM + EA)

The NDVI trend shows a dip in 2020 and 2021 (figure 3.5.4 and 3.5.5) and then flourishing flora during the next years. This is reflected in the band trend series as seen in Figure 3.5.3 where during the year 2022 there is rapid increase in reflectance for RE and NIR bands. The seasonal NDVI analysis, figure 3.5.6 shows that the species health is highest during October – December months. In the year 2021 the NDVI values of all the species gone down considerably. The NDVI value for AO is lowest followed by AA.

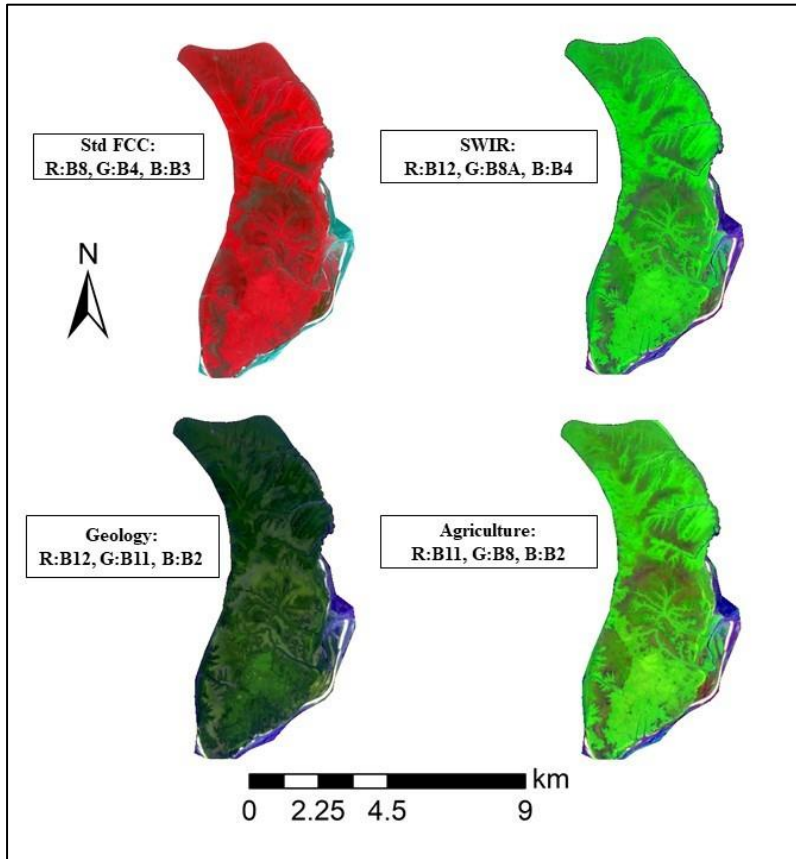


Figure 3.5.1 Color composites of Lothian Island study site.

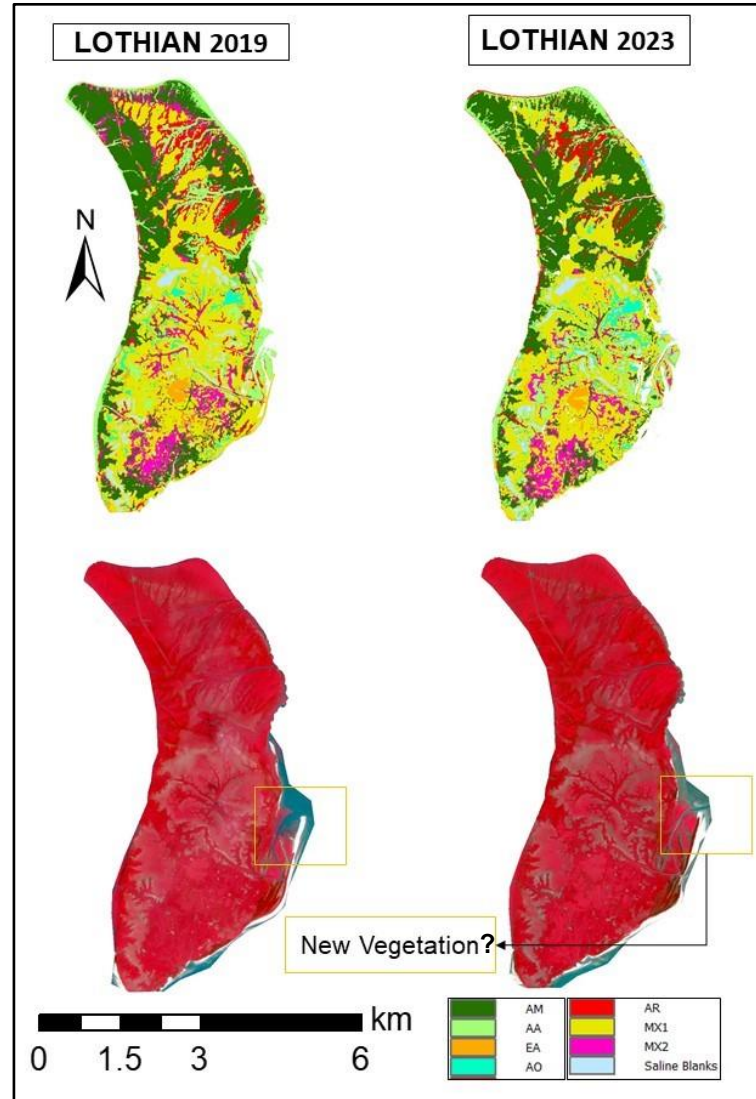


Figure 3.5.2 Classification outputs using RF for February 2019 and February 2023 for Lothian Island site.

Table 3.5.1 Accuracy assessment: Lothian Island

Random Forest classifier	Overall accuracy	Kappa coefficient
Initial image (Feb 2019)	0.99	0.98
Final image (Feb 2023)	0.98	0.97

Table 3.5.2 JM distance matrix for Lothian Island.

	AM	AA	EA	AO	AR	MX1	MX2
AM	-	1.93	2.0	1.99	1.99	1.85	1.79
AA	1.93	-	2.0	2.0	1.99	1.99	1.99
EA	2.0	2.0	-	2.0	2.0	1.99	1.99
AO	1.99	2.0	2.0	-	2.0	1.99	2.0
AR	1.99	1.99	2.0	2.0	-	1.99	1.99
MX1	1.85	1.99	1.99	1.99	1.99	-	1.85
MX2	1.79	1.99	1.99	2.0	1.99	1.85	-

Table 3.5.3 Land cover of different mangrove species: Lothian Island.

	Initial area (km ²)	Final area (km ²)
<i>Avicennia marina</i>	9.46	10.54
<i>Avicennia alba</i>	3.96	4.23
<i>Excoecaria agallocha</i>	0.47	0.41
<i>Avicennia officinalis</i>	0.91	1.55
<i>Aegialitis rotundifolia</i>	2.05	1.62
MX1	13.48	11.65
MX2	3.16	2.05
Saline blanks	1.16	1.33

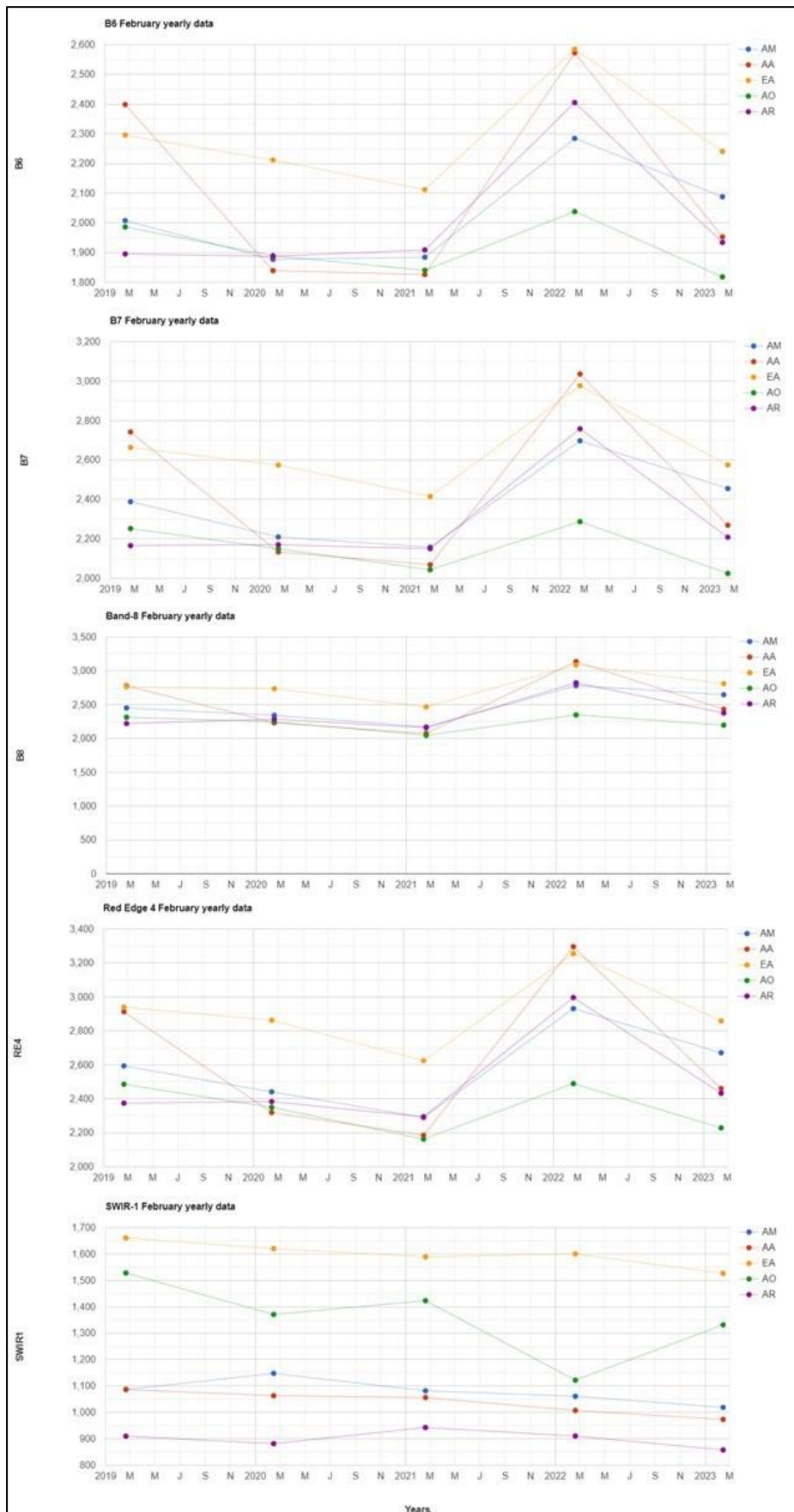


Figure 3.5.3. Yearly data of February 2019 - 2023 for Band 6, Band 7, Band 8, Band 8A, Band 11 for Lothian Island.

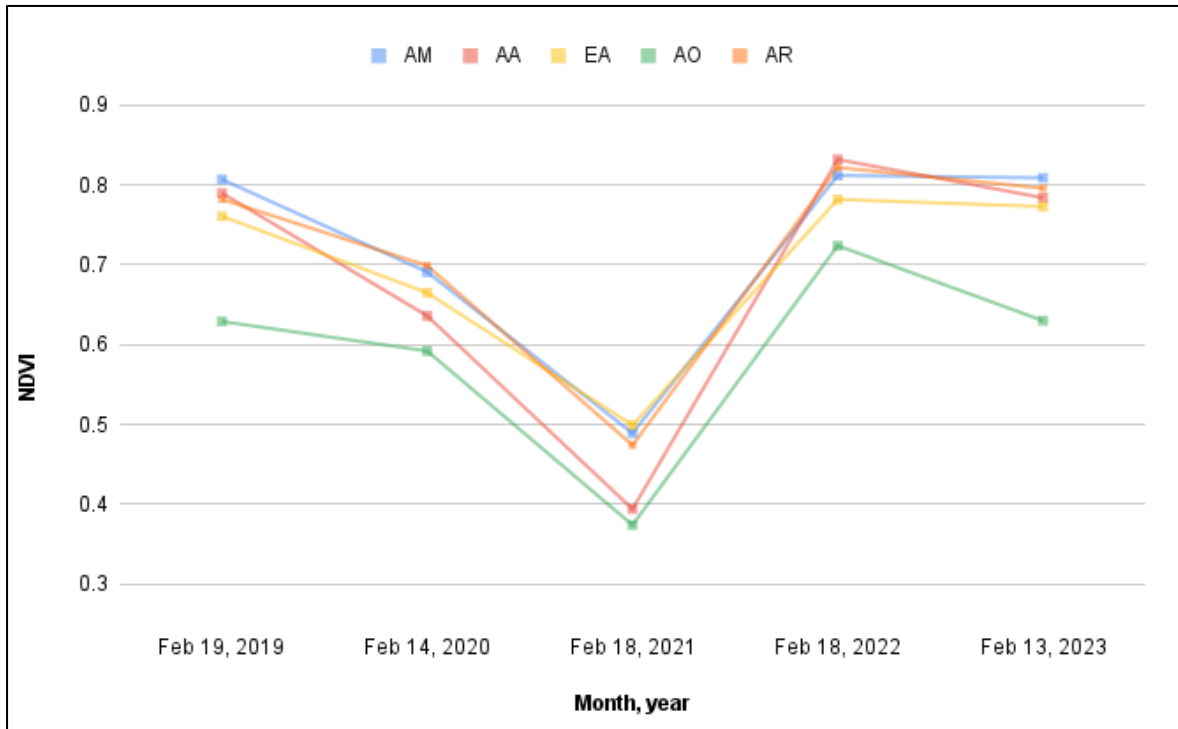


Figure 3.5.4. NDVI yearly trend for February from 2019-2023 for Lothian Island.

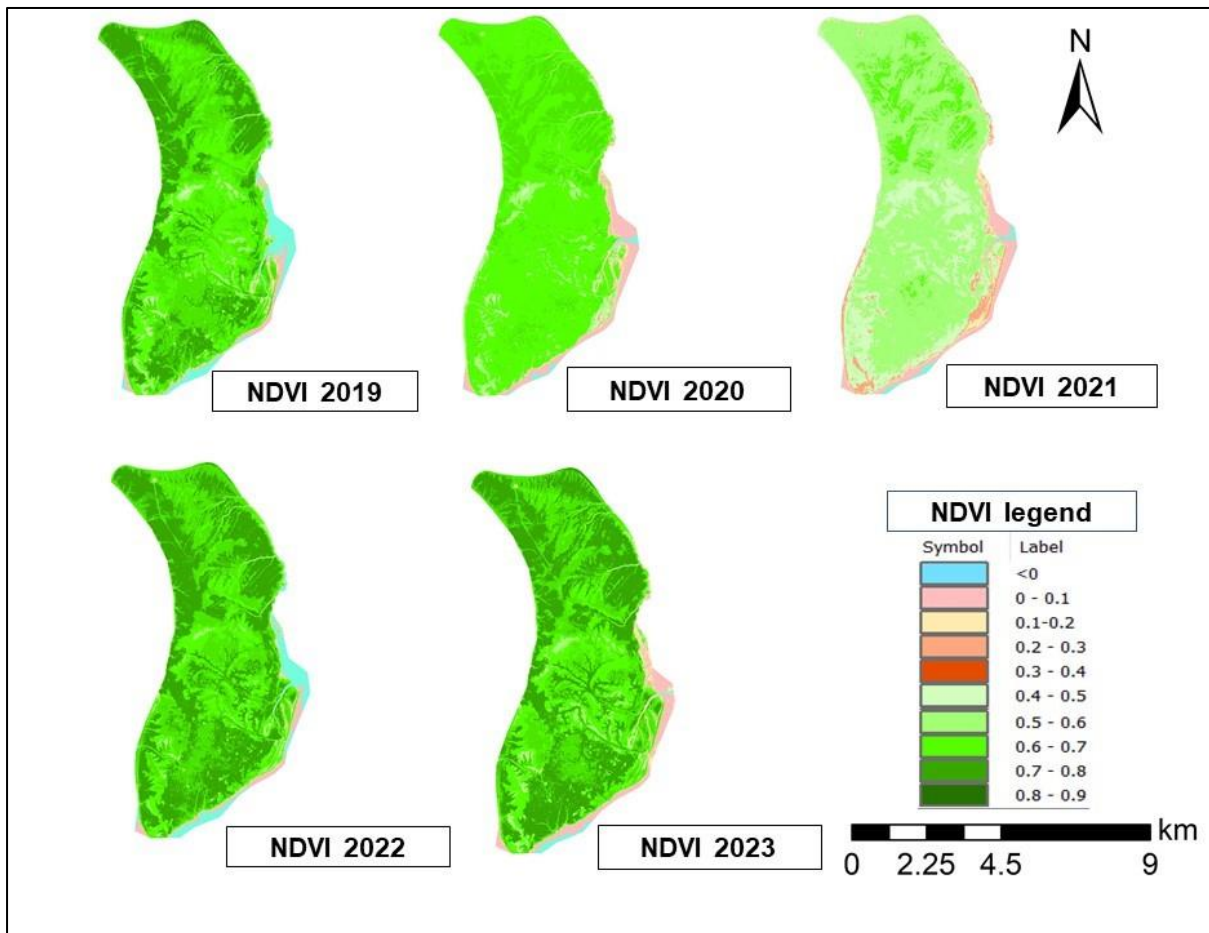


Figure 3.5.5. NDVI image of February 2019 – 2023 with range for Lothian Island.

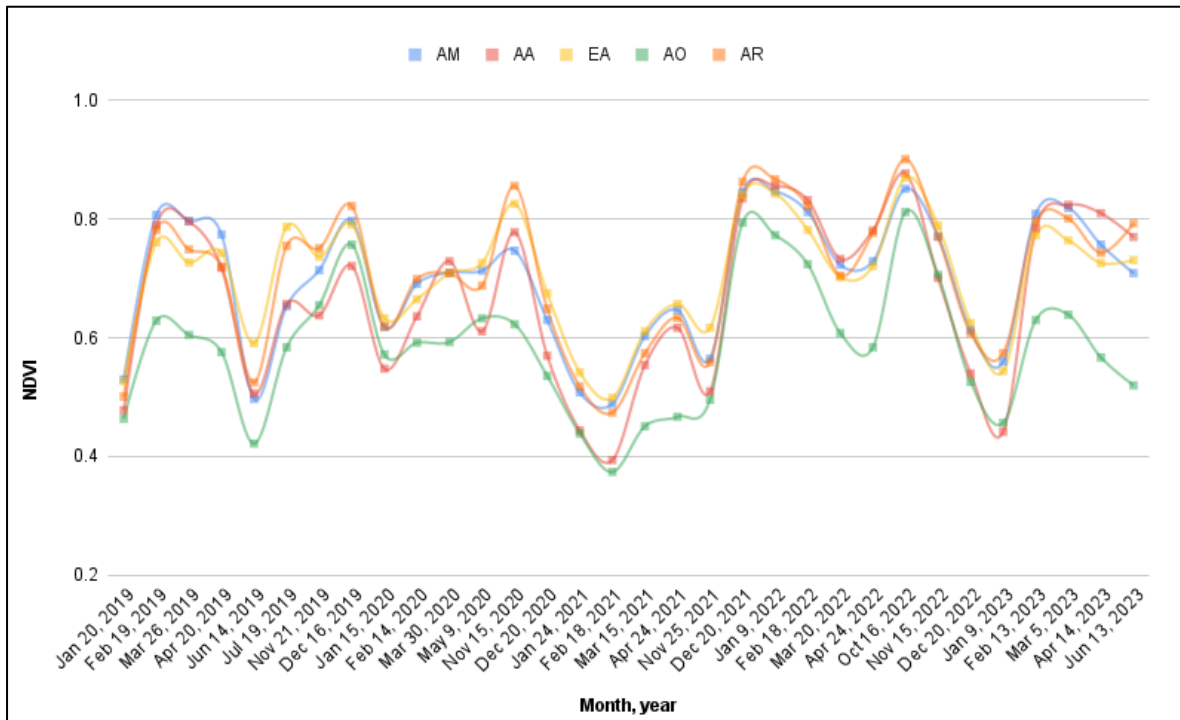


Figure 3.5.6. NDVI seasonal trend from 2019 – 2023 for each species of Lothian Island.

3.6 Pichavaram

Pichavaram study site has an area of 10.16 km². It lies in the East coast of India. This region is dominated by *Avicennia marina* (AM) species. With the preliminary analysis, figure 3.3.1, no much information could be derived. The vegetation seems to be in homogenous patches. In some areas there is mud interior to the land, and the vegetation surrounding these regions could be seen as sparsely populated.

For the classification, the spectral separability JM matrix indicates that all the species classes considered have good separability (table 3.6.2). Classification outputs, figure 3.6.2 of this region shows some region occupied by AM dense have been converted to soil. While inspecting the area change, table 3.6.3 it is observed that the soil or land area has increased from 0.84 to 1.32 km². Among mangrove species, AM sparse patches has increased and *Rhizophora sp.* (RH) has decrease.

The NDVI seasonal trend, figure 3.6.4 shows that AM dense has higher NDVI values, followed by AM sparse and RH. During the January – February duration the vegetation health seems to be the lowest in a year. From figure 3.6.5 it could be seen that the vegetation health for month of March for five years from 2016 shows

cyclical changes. The vegetation is most healthy during the year 2016, and although it the health decreases for the next year same season, by 2023 it has regained health.

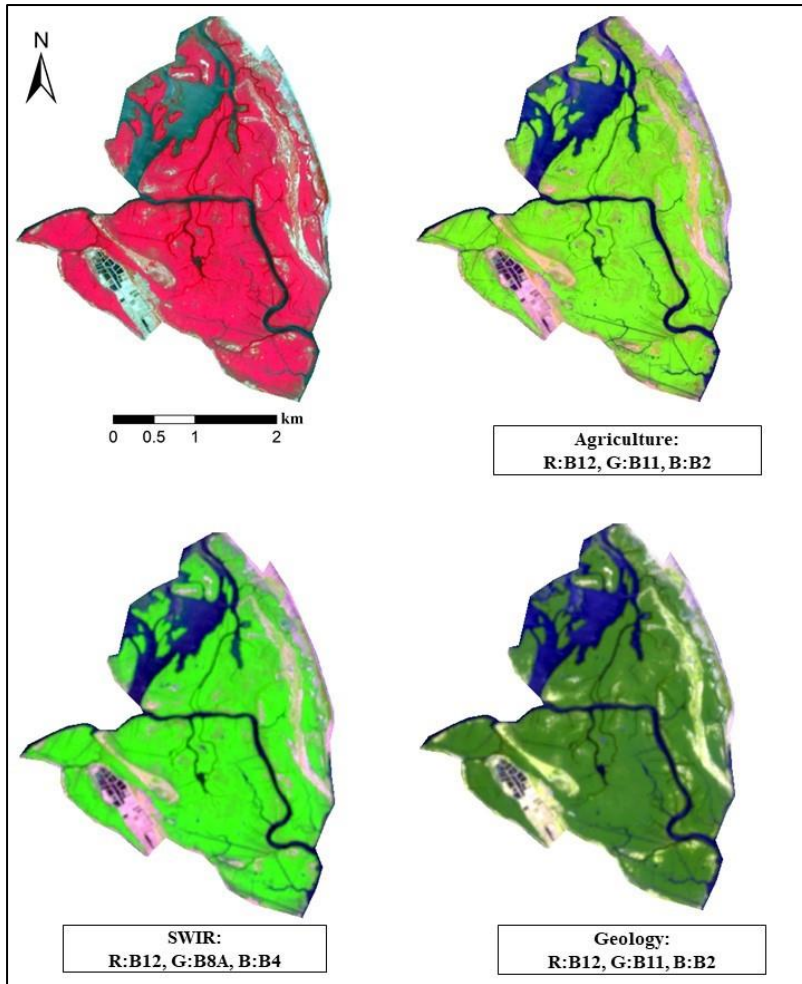


Figure 3.6.1. Different band combinations for Pichavaram study site. Image with scale and North arrow is standard FCC.

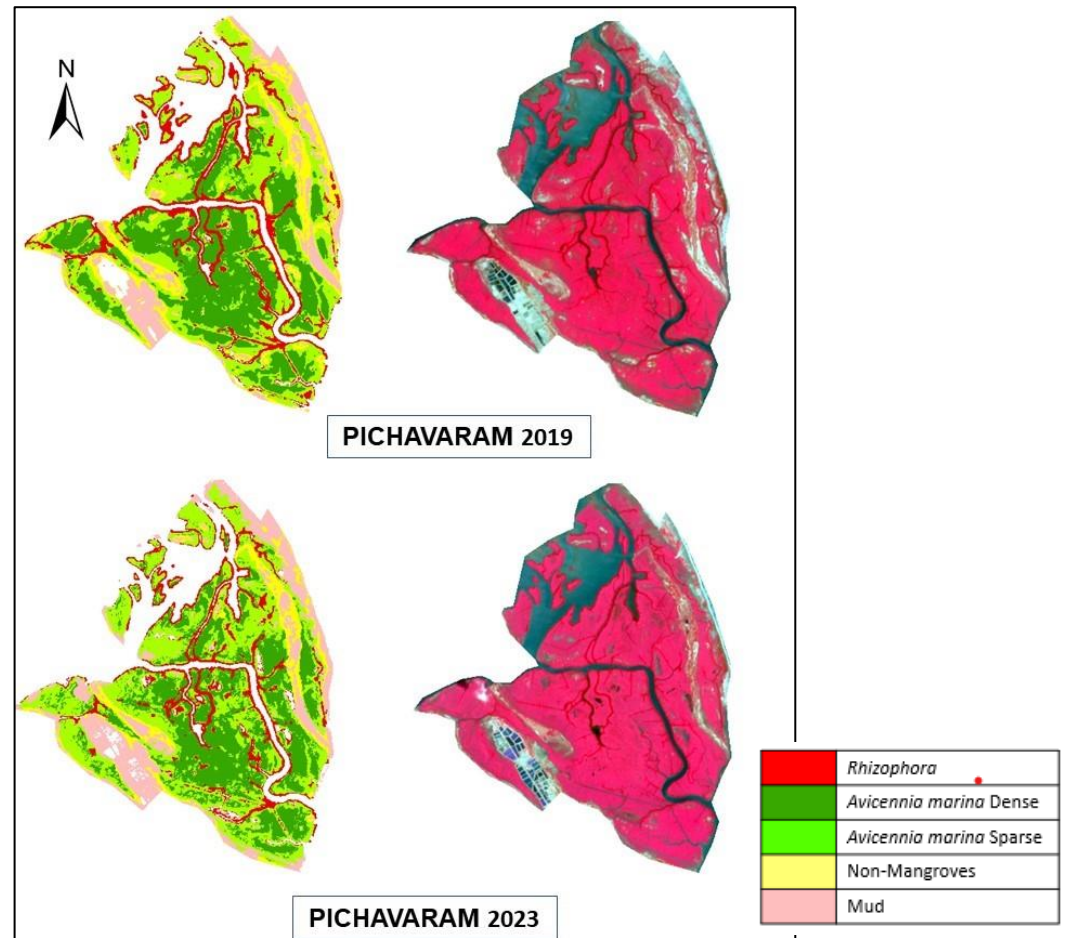


Figure 3.6.2. Classification output for Pichavaram site.

Table 3.6.1 Accuracy assessment: Pichavaram

Random Forest classifier	Overall accuracy	Kappa coefficient
Initial image (27 th March 2019)	0.99	0.99
Final image (16 th March 2023)	0.99	0.99

Table 3.6.2. JM distance matrix for Pichavaram.

Class	RH	AM_sparse	AM_dense	Non-Mangroves
RH	–	1.97	1.99	1.99
AM_sparse	1.97	–	1.97	1.99
AM_dense	1.99	1.97	–	1.99
Non-Mangroves	1.99	1.99	1.99	–

Table 3.6.3 Land cover of different mangrove species: Pichavaram.

	Initial area (km ²)	Final area (km ²)
Water	1.40	1.25
Soil	0.84	1.32
<i>Rhizophora sp.</i>	1.45	1.04
<i>Avicennia marina</i> Dense	2.70	2.43
<i>Avicennia marina</i> Sparse	2.69	3.20
Terrestrial vegetation	0.92	0.56

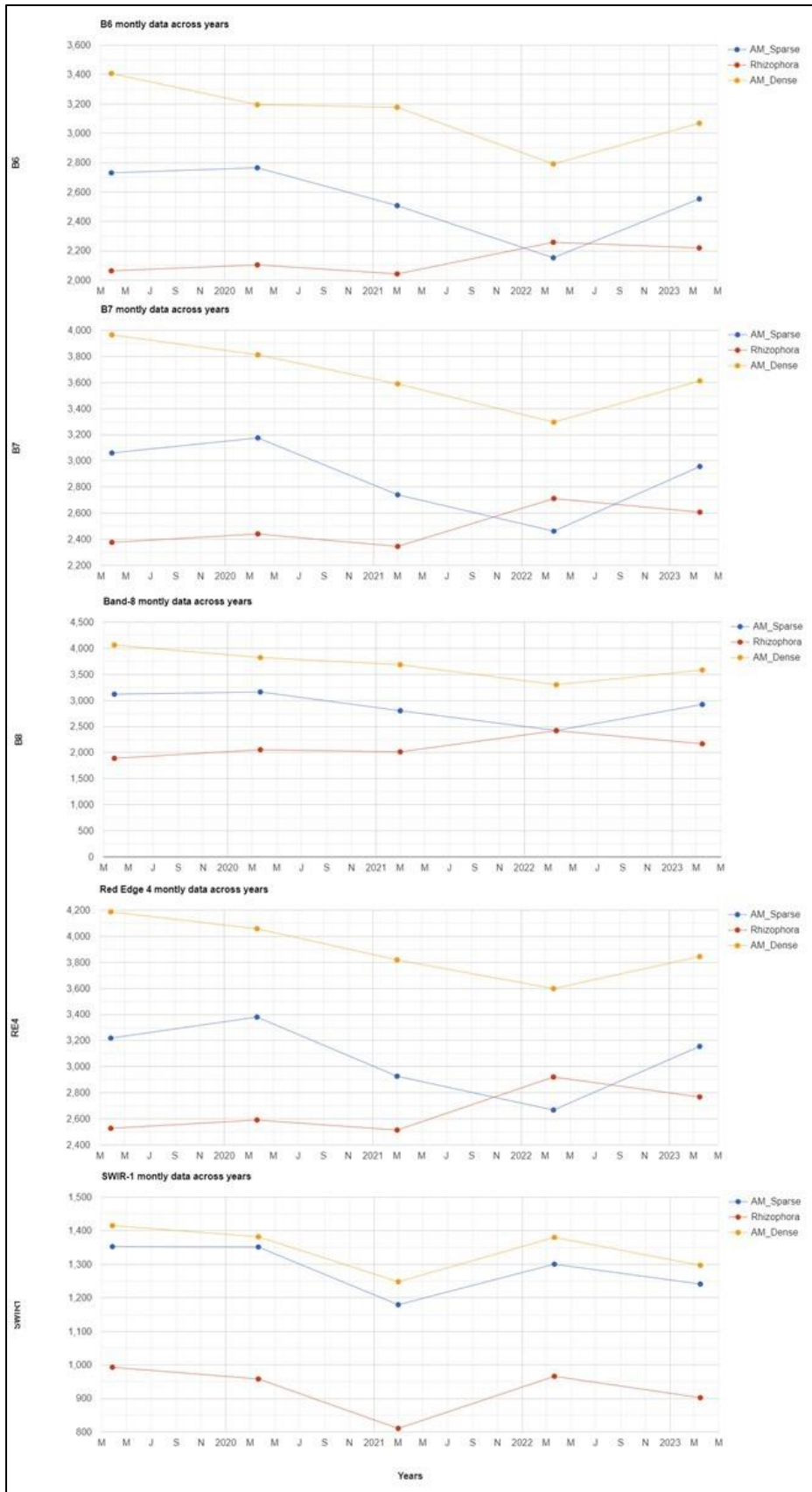


Figure 3.6.3. Yearly data of March 2019 - 2023 for Band 6, Band 7, Band 8, Band 8A, Band 11 for Pichavaram.

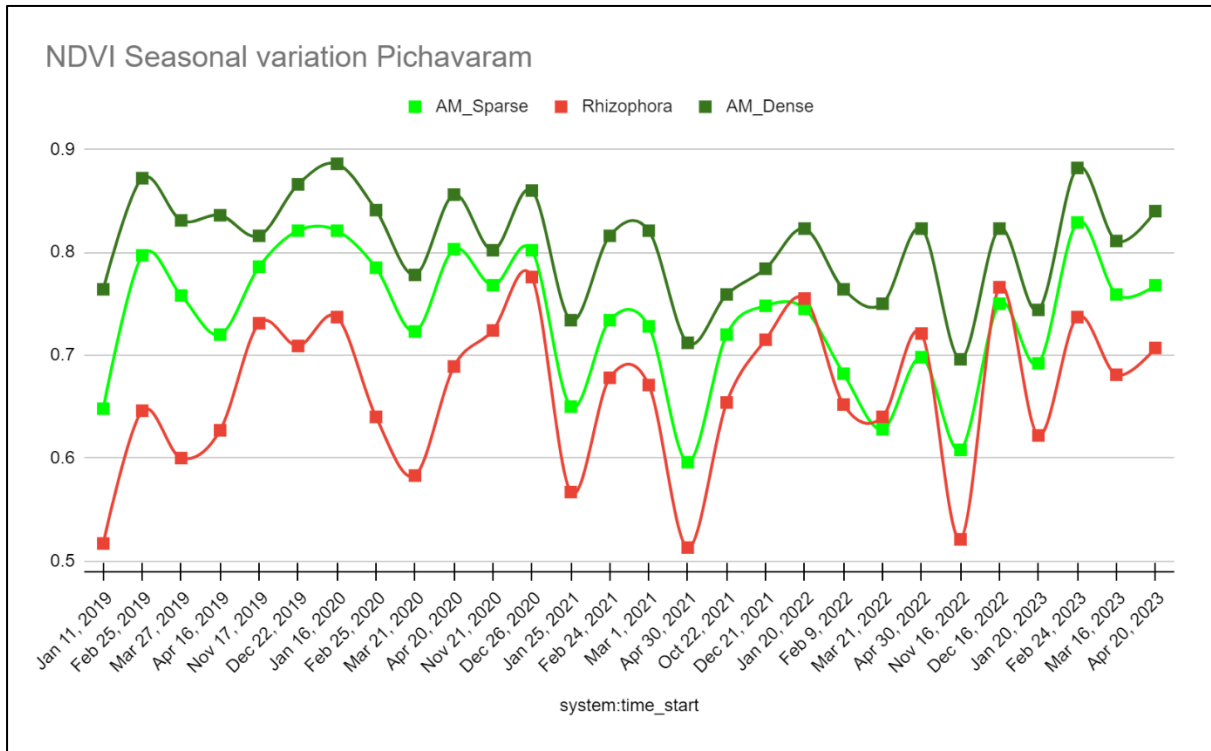


Figure 3.6.4. NDVI seasonal trend from 2019 – 2023 for each species of Pichavaram.

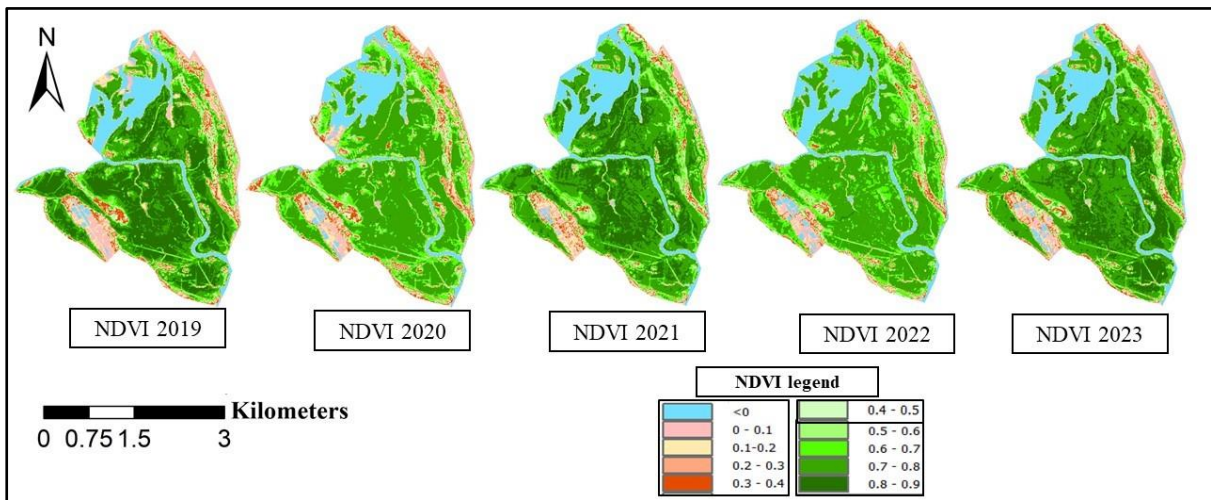


Figure 3.6.5. NDVI image of March 2016 – 2022 with range for Pichavaram.

3.7 Malad

Malad study site, lying along the west coast of India has an area of 10.80 km². This region has *Avicennia marina* (AM) and *Rhizophora mucronate* (RM). From the preliminary analysis by different band combinations, figure 3.7.1 it can be seen clear that there are more than one mangrove species present in the region. For the

classification, the JM separability criteria was met as the values was all >1.8 , and it is tabulated in table 3.7.2.

From the classification output (Figure 3.7.2), the region has AM and RM mangroves and it is seen there is decrease in the RM extend by 0.16 km^2 . There is also decrease in the extent of AM species, which decreased by 0.9 km^2 . There is a substantial increase in mud region, from 0.71 to 1.92 km^2 , which would have taken the previously present mangrove species.

Yearly band values (Figure 3.7.3) for NIR and RE does not show any evidence of particular disturbance in its trend. Overall NDVI seems to be on the rise as we can see from Figure 3.7.4 , and that is validated through figure 3.7.5. It is observed that during each year, the vegetation is at its peak health during the month of March.

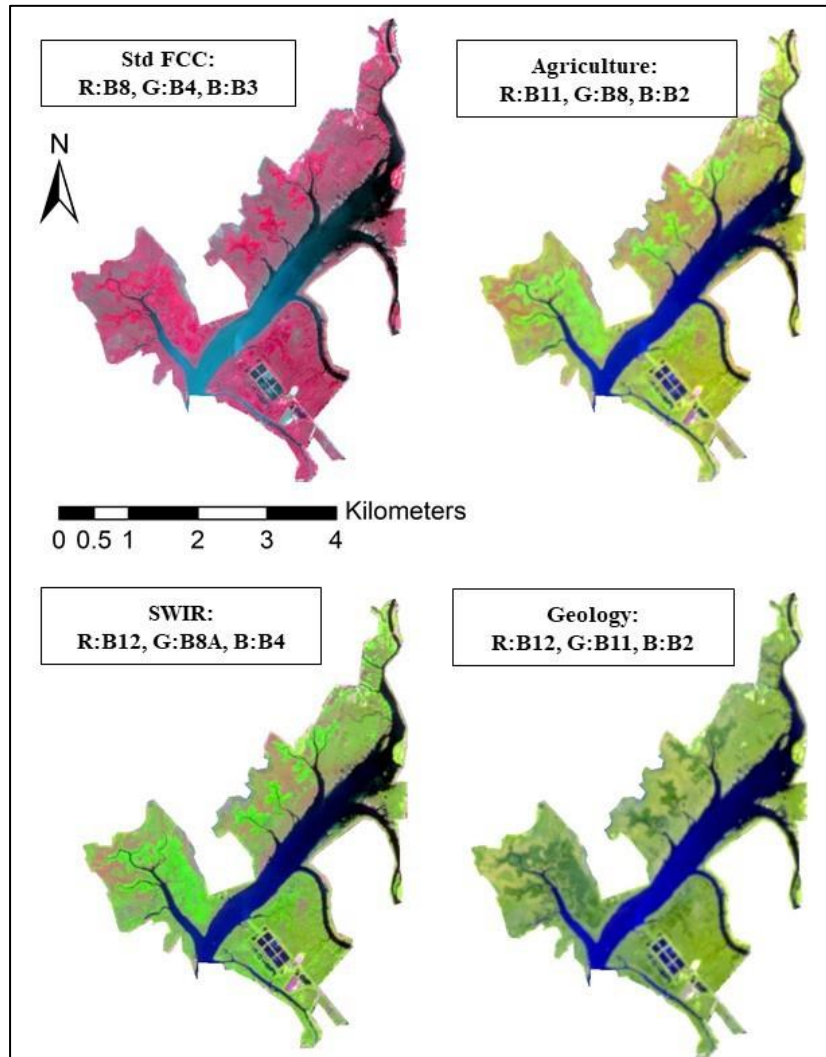


Figure 3.7.1. Different band combinations for Malad study site.

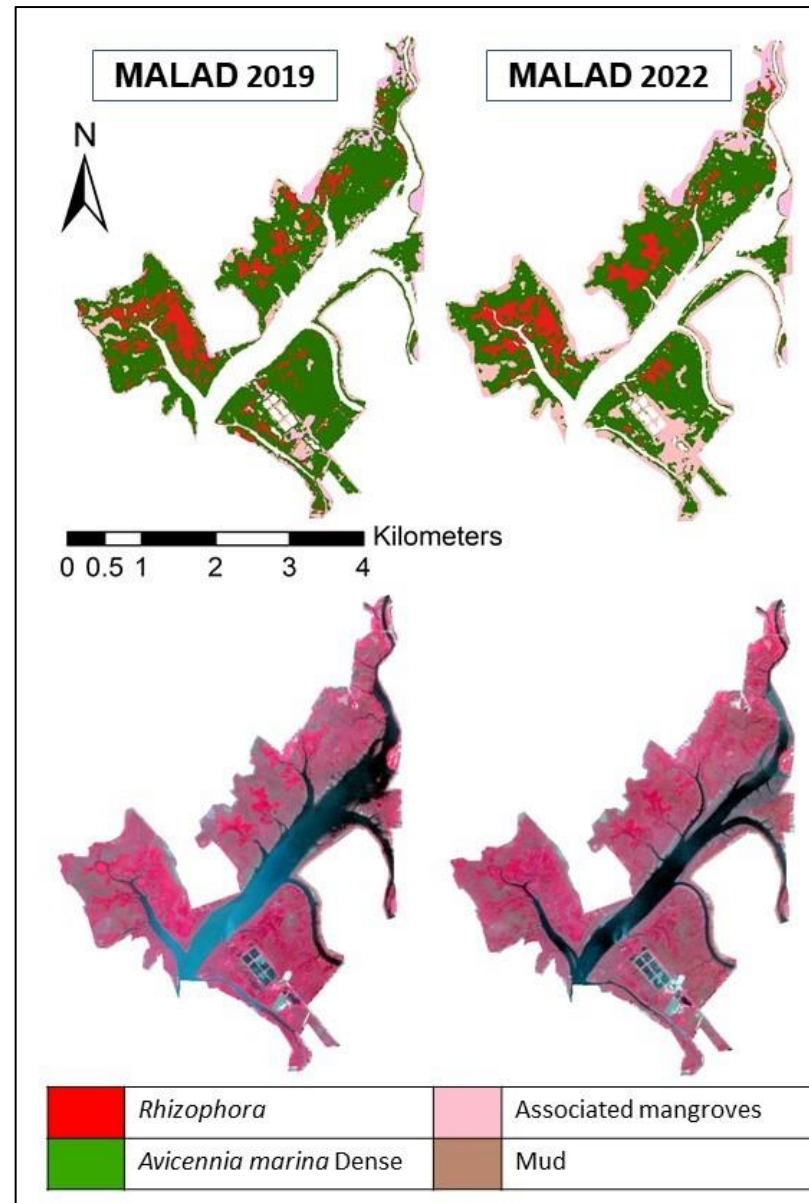


Figure 3.7.2. Classification outputs for Malad site.

Table 3.7.1 Accuracy assessment: Malad.

Random Forest classifier	Overall accuracy	Kappa coefficient
Initial image (14 th Nov 2019)	0.99	0.98
Final image (13 th Nov 2022)	0.98	0.97

Table 3.7.2. JM distance matrix for Malad.

	RH	AM	Associated Mangroves
RH	–	1.99	1.99
AM	1.99	–	1.99
Associated Mangroves	1.99	1.99	–

Table 3.7.3 Land cover of different mangrove species: Malad region.

	Initial area (km ²)	Final area (km ²)
<i>Rhizophora sp.</i>	1.02	0.86
<i>Avicennia marina</i>	5.91	5.01
Associated Mangroves	0.61	0.48
Mud	0.71	1.92
water	2.42	2.4

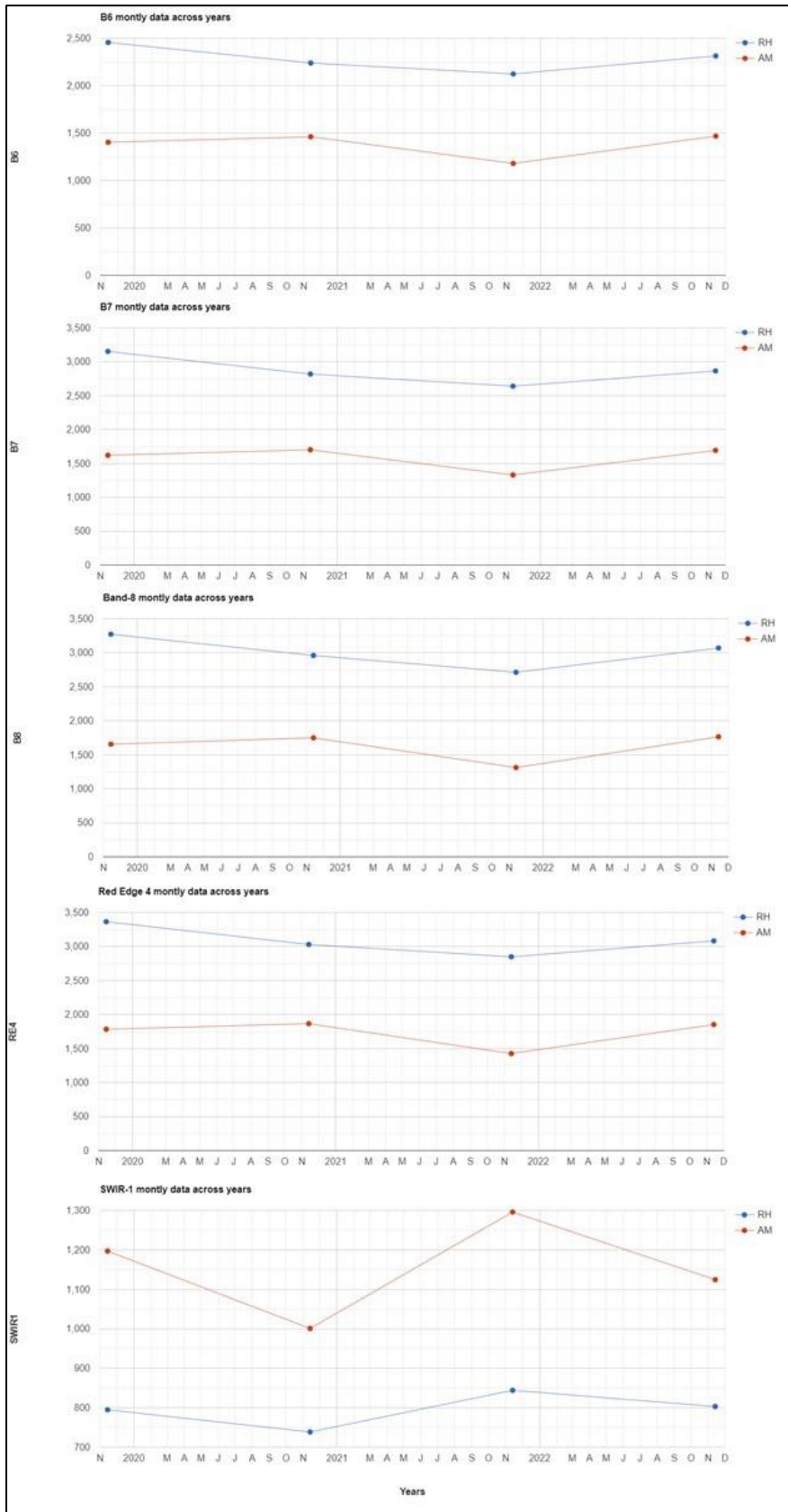


Figure 3.7.3. Yearly data of November 2019 - 2023 for Band 6, Band 7, Band 8, Band 8A, Band 11 for Malad site.

NDVI analysis:

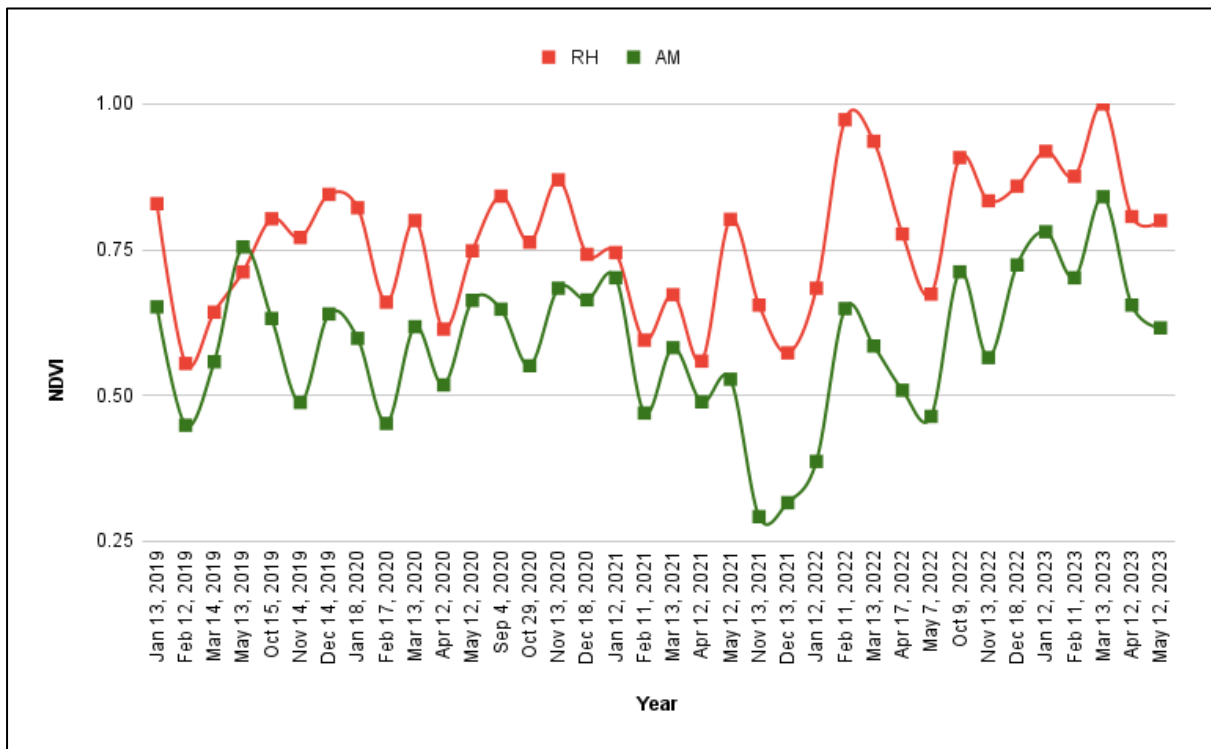


Figure 3.7.4. NDVI seasonal trend from 2019 – 2023 for each species of Malad.

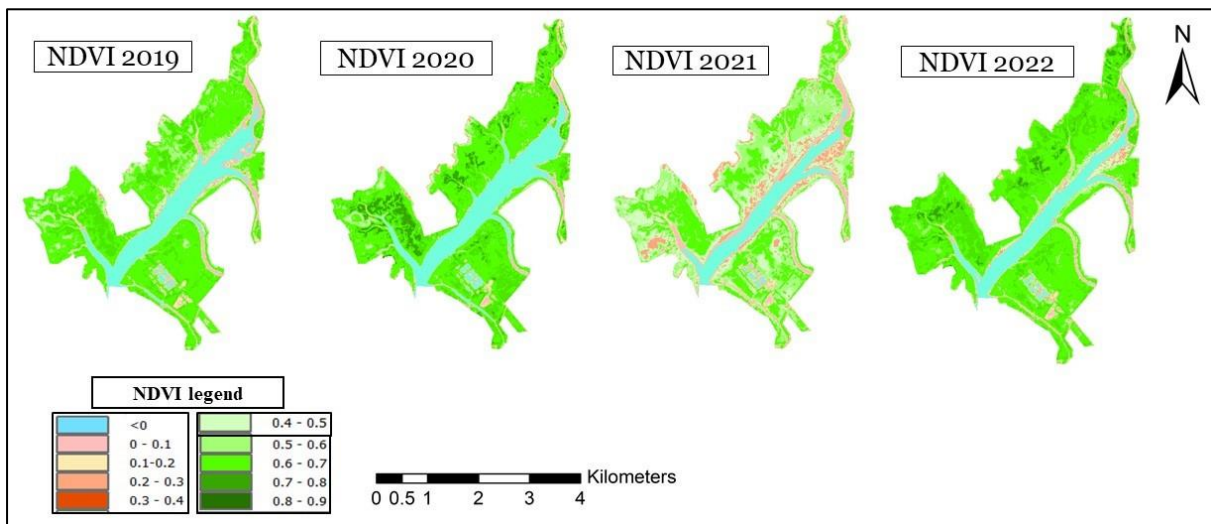


Figure 3.7.5. NDVI image of November 2019 – 2022 with range for Malad.

Chapter 4 Conclusion

The study successful in mapping and monitoring the mangrove species of the coastal regions the study was conducted on. The species diversity in the East coast mangrove forests is higher in comparison to West coast forests, that has been reported from previous different studies, and it was confirmed with the study carried out. *Avicennia marina*, *Rhizophora sp.* and *Sonneratia sp.* are the mangroves that were identified in the west coast study sites while in the east coast the mangrove species included *Avicennia sp*, *Aegialitis rotundifolia*, *Heritiera fomes* and *Excoecaria agallocha* among the other species found from west coast.

The remote sensing approach provides an alternative way to traditional onsite field surveys, which is difficult to inaccessible areas such as these mangrove forests. Multi time field visits are also not feasible, as explained by Eric (Eric et al. 2017), where these remote sensing approaches becomes resourceful.

The exceptionally good spatial resolution of multispectral Sentinel-2 data has enabled in identifying mangroves at a species level, where conventionally hyperspectral satellite data is used. In the study regions of Thane, Pichavaram and Malad, the mangrove vegetation has decreased in the study time and the vegetation patches are replaced by mud deposition. The mangrove vegetation in the East coast are highly heterogenous comparatively, hence it is possible for the presence of misclassification. In the Bhitarkanika region 2022 classification image, the decreased HF sparse population region is dominated by mixed mangroves. These assessments needs to be verified with very high resolution airborne satellite data or field surveys as some of the mangrove species in the Bhitarkanika forest are endangered species and a reduction in its population is a matter of concern. Within the study span of 5 years, there are new vegetation patches of mangroves detected in the Indian Sundarban region, Lothian Island. These indicates the rapid rate of mangrove colonization in those fertile soils.

During fieldwork, the canopy reflectance hyperspectral data collected for mangroves gives the species spectral differences. This data could be used as the reference spectrum for further studies using supervised classification algorithms such as the spectral angle mapper or spectral information divergence. Conventionally these

algorithms are utilized for hyperspectral image classifications. Prior to visiting a field location, an integral study of study site has to be done to get insight on which time of year the satellite images are cloud free, and when the study site have summer season. This has been followed throughout the study conducted, and the seasonal variations to the vegetation are traced through the NDVI changes in the study areas. Further upon field visits it was observed that the low tide time of day should be utilized for field operations and highly accurate GPS instruments should be carried as GPS on the mobile phones have low accuracy in remote areas.

Limitations:

- For locations of Bhitarkanika, Sadamirya and Thane the satellite images are not atmospherically corrected. Further, these could not be processed with the sen2cor algorithm in SNAP software as these were downloaded from GEE platform.
- The cloud cover in monsoon time over the study areas have limited the conclusion of vegetation health analysis to only cloud free months of year. This could be mitigated with the use of sentinel 1, Synthetic Aperture Radar remote sensing.
- Limited spectral resolution of Sentinel 2 imagery affects the land cover identification.

References

Abdul Azeez S., Gnanappazham L., Muraleedharan K.R., Revichandran C., Sebin John, Seena G., Jubin Thomas, Multi-decadal changes of mangrove forest and its response to the tidal dynamics of thane creek, Mumbai, Journal of Sea Research, Volume 180, 2022, 102162, ISSN 1385-1101, <https://doi.org/10.1016/j.seares.2021.102162>.

Alvin B. Baloloy, Ariel C. Blanco, Raymund Rhommel C. Sta. Ana, Kazuo Nadaoka, Development and application of a new mangrove vegetation index for rapid and accurate mangrove mapping, ISPRS Journal of Photogrammetry and Remote Sensing, Volume 166, 2020, ISSN 0924-2716, <https://doi.org/10.1016/j.isprsjprs.2020.06.001>.

Campos-Taberner, M.; García-Haro, F.J.; Martínez, B.; Sánchez-Ruiz, S.; Gilabert, M.A. A Copernicus Sentinel-1 and Sentinel-2 Classification Framework for the 2020+ European Common Agricultural Policy: A Case Study in València (Spain). *Agronomy* 2019, 9, 556. <https://doi.org/10.3390/agronomy9090556>

Chaube, Nilima R., Nikhil Lele, Arundhati Misra, T. V. R. Murthy, Sudip Manna, Sugata Hazra, Muktipada Panda, and R. N. Samal. "Mangrove Species Discrimination and Health Assessment Using AVIRIS-NG Hyperspectral Data." *Current Science* 116, no. 7 (2019): 1136–42. <https://www.jstor.org/stable/27138005>.

Eric L. Bullock, Sergio Fagherazzi, William Nardin, Phuoc Vo-Luong, Phong Nguyen, Curtis E. Woodcock, Temporal patterns in species zonation in a mangrove forest in the Mekong Delta, Vietnam, using a time series of Landsat imagery, <https://doi.org/10.1016/j.csr.2017.07.007>.

FieldSpec® 3 User Manual (ASD 2010)

G. Viennois et al., "Multitemporal Analysis of High-Spatial-Resolution Optical Satellite Imagery for Mangrove Species Mapping in Bali, Indonesia," in *IEEE Journal*

of Selected Topics in Applied Earth Observations and Remote Sensing, vol. 9, no. 8, pp. 3680-3686, Aug. 2016, doi: 10.1109/JSTARS.2016.2553170.

H. Jeffreys, "An Invariant for the Prior Probability in Estimation Problems," Proc. Roy. Soc. A., Vol. 186, pp. 454-461, 1946.

H. Sanam, A. K. Mathai and G. Lakshmanan, "Multi-resolution remote sensing for the species level classification of mangroves," 2023 International Conference on Machine Intelligence for GeoAnalytics and Remote Sensing (MIGARS), Hyderabad, India, 2023, pp. 1-4, doi: 10.1109/MIGARS57353.2023.10064566.

Hueni, Andreas & Bialek, Aga. (2017). Cause, Effect, and Correction of Field Spectroradiometer Interchannel Radiometric Steps. IEEE Journal of Selected Topics in Applied Earth Observations and Remote Sensing. PP. 1-10.
10.1109/JSTARS.2016.2625043.

J.A. Richards, 1999, Remote Sensing Digital Image Analysis, Springer-Verlag, Berlin, p. 240.

Jyoti Prakash Hati, Sourav Samanta, Nilima Rani Chaube, Arundhati Misra, Sandip Giri, Niloy Pramanick, Kaushik Gupta, Sayani Datta Majumdar, Abhra Chanda, Anirban Mukhopadhyay, Sugata Hazra, Mangrove classification using airborne hyperspectral AVIRIS-NG and comparing with other spaceborne hyperspectral and multispectral data, The Egyptian Journal of Remote Sensing and Space Science, Volume 24, Issue 2, 2021, Pages 273-281,ISSN 1110-9823,
<https://doi.org/10.1016/j.ejrs.2020.10.002>.

K, ripa & Mudaliar, Ashwini & Lele, Nikhil & Mankad, Archana & Murthy, Tvr. (2019). Spatio-Temporal Variations in Mangrove Vegetation in conjunction with Related Environmental Factors in Pichavaram (India) 1996-2016. International Journal of Scientific Research in Biological Sciences. 6. 15-25. 10.26438/ijrsbs/v6i2.1525.

Lakshmanan, Gnanappazham & Selvam, V.. (2014). Response of mangroves to the change in tidal and fresh water flow – A case study in Pichavaram, South India. Ocean & Coastal Management. 102. 131–138. 10.1016/j.ocecoaman.2014.09.004.

Luetzenburg, G., Kroon, A. & Bjørk, A.A. Evaluation of the Apple iPhone 12 Pro LiDAR for an Application in Geosciences. *Sci Rep* 11, 22221 (2021).
<https://doi.org/10.1038/s41598-021-01763-9>

M. Dabboor, S. Howell, M. Shokr & J. Yackel (2014) The Jeffries–Matusita distance for the case of complex Wishart distribution as a separability criterion for fully polarimetric SAR data, *International Journal of Remote Sensing*, 35:19, 6859-6873, DOI: 10.1080/01431161.2014.960614

Mai NT, Huong TTL, Dat TT, Truong DD. An Empirical Study of Financial Efficiency and Stability of Shrimp–Mangrove Farming Model in Nam Dinh Province, Red River Delta, Vietnam. *Sustainability*. 2023; 15(7):6062. <https://doi.org/10.3390/su15076062>

Mulla, Tarnnum & Chavan, Niranjana. (2017). Mangrove Diversity along the Coast of Ratnagiri, Maharashtra. *Current Botany*. 8. 10.19071/cb.2017.v8.3225.

Nagarajan, P., Rajendran, L., Pillai, N.D. et al. Comparison of machine learning algorithms for mangrove species identification in Malad creek, Mumbai using WorldView-2 and Google Earth images. *J Coast Conserv* 26, 44 (2022).
<https://doi.org/10.1007/s11852-022-00891-2>

P. V. Janse, J. N. Kayte, R. V. Agrawal and R. R. Deshmukh, "Standard Spectral Reflectance Measurements for ASD FieldSpec Spectroradiometer," 2018 Fifth International Conference on Parallel, Distributed and Grid Computing (PDGC), Solan, India, 2018, pp. 729-733, doi: 10.1109/PDGC.2018.8745808.

Padma, S. and Sanjeevi, S., Jeffries Matusita-Spectral Angle Mapper (JM-SAM) spectral matching for species level mapping at Bhitarkanika, Muthupet and Pichavaram mangroves, *ISPRS - International Archives of the Photogrammetry, Remote Sensing and Spatial Information Sciences*. DOI:10.5194/isprsarchives-XL-8-1403-2014

Padmakumar, Vidya & S., Murugan. (2022). Mangrove ecology and species distribution along the Gorai Creek of Mumbai coast, Maharashtra, India. 6. 22-26. 10.22161/ijfaf.6.4.4.

Pandisamy, Ragavan & Saxena, Alok & Jayaraj, Rsc & Mohan, P.M. & Ravichandran, Karuppiyah & Saravanan, Ketharanathan & VIJAYARAGHAVAN, A.. (2016). A review of the mangrove floristics of India. *Taiwania*. 61. 224-242. 10.6165/tai.2016.61.224.

Pillai, Neethu & C C, Harilal. (2018). MANGROVES – A REVIEW. 5. 4035-4038. Saintilan, N., Horton, B., Törnqvist, T.E. et al. Widespread retreat of coastal habitat is likely at warming levels above 1.5 °C. *Nature* 621, 112–119 (2023). <https://doi.org/10.1038/s41586-023-06448-z>

Yancho, J.M.M.; Jones, T.G.; Gandhi, S.R.; Ferster, C.; Lin, A.; Glass, L. The Google Earth Engine Mangrove Mapping Methodology (GEEMMM). *Remote Sens.* 2020, 12, 3758. <https://doi.org/10.3390/rs12223758>